WMRC Reports
Waste Management and Research Center

# Demonstration of Hydraulic Fracturing to Facilitate Remediation

Larry Murdoch,
Mark Kemper,
Mohan Narayanaswamy,
Allen Wolf

University of Cincinnati

RR-E68
April 1994
Electronic Version

## About WMRC's Electronic Publications:

This document was originally published in a traditional format

It has been transferred to an electronic format to allow faster and broader access to important information and data

While the Center makes every effort to maintain a level of quality during the transfer from print to digital format, it is possible that minor formatting and typographical inconsistencies will still exist in this document

Additionally, due to the constraints of the electronic format chosen, page numbering will vary slightly from the original document

The original, printed version of this document may still be available

Please contact WMRC for more information

**WMRC**
**One E. Hazelwood Drive**
**Champaign, IL 61820**
**217-333-8940 (phone)**

**www.wmrc.uiuc.edu**


WMRC is a division of the Illinois Department of Natural Resources

Hazardous Waste Research and Information Center
One East Hazelwood Drive
Champaign, Illinois 61820

*HWRIC RR-068* *$5 00*

# Demonstration of Hydraulic Fracturing to Facilitate Remediation

by

Larry Murdoch, Mark Kemper,
Mohan Narayanaswamy
and Allen Wolf
University of Cincinnati
Center for GeoEnvironmental Science and Technology

April 1994
*Printed on recycled/recyclable paper*


HWRIC RR-068

# Demonstration of Hydraulic Fracturing to Facilitate Remediation

by

Larry Murdoch, Mark Kemper
Mohan Narayanaswamy
and Allen Wolf
University of Cincinnati
Center for GeoEnvironmental Science and Technology

Prepared for

Hazardous Waste Research and Information Center
One East Hazelwood Drive
Champaign, Illinois 61820

HWRIC Project Number HWR-91-090

Printed by Authority of the State of Illinois

94/250

This report is part of HWRIC's Research Report Series  Mention of trade names or commercial products does not constitute endorsement or recommendation for use.

## Acknowledgments

This research has been supported by the Hazardous Waste Research and Information Center in Champaign, Illinois In addition, we received support and guidance from the United States Environmental Protection Agency's Risk Reduction Engineering Laboratory in Cincinnati, Ohio We would also like to thank our colleagues at the University of Cincinnati's Center for GeoEnvironmental Science and Technology for their contributions

## Table of Contents

## List of Tables

## List of Figures

## Abstract

Sand-filled hydraulic fractures were created at three sites to investigate their effect on in situ remedial efforts At a site contaminated with volatile organic compounds, fractures were created to enhance the effectiveness of soil vapor extraction (SVE), whereas at another site contaminated with diesel fuel, hydraulic fractures were created to improve the rate of delivery of nutrients for in-situ bioremediation Another site, which was uncontaminated, was utilized to study air flow in the vicinity of hydraulic fractures All of the sites were underlain by overconsolidated silty clay glacial drift

Conventional wells were installed at each of the sites to act as controls and comparisons were made between the performance of fractured and conventional wells Comparisons of well discharge, suction head distribution, and contaminant mass removal rates were made at the SVE sites Comparisons of injection rates, pressure head distribution, bioactivity, soil moisture, and biodegradation rate were made at the bioremediation site

Results indicate that hydraulic fractures increase the recovery rates and area affected by SVE During SVE, volumetric discharge and mass recovery rates from fractured wells were roughly an order of magnitude greater than those from conventional wells In addition, the areas affected (as indicated by suction in the subsurface) increased from less than 1 5 m from a conventional well to more than 6 10 m from a fractured well Similar changes in volumetric discharge and area affected by a well were observed at the contaminated and uncontaminated sites

The fractures also improved the performance of bioremediation The rate of injection of a solution of hydrogen peroxide and nutrients into a fractured well was two orders of magnitude greater than into a conventional injection well Soil moisture content, bioactivity, and the rate of degradation of BTE in the vicinity of the fractured well was also greater than in the vicinity of the unfractured well

# 1.0 Introduction

## 1.1 Background

In situ methods of removing contaminants from soil can reduce costs and limit additional exposure to the contaminants The effectiveness of in situ remedial technologies that require fluid flow through the subsurface (e g pump and treat, soil vapor extraction, and bioremediation), however, is often limited by the permeability of the formation Consequently, sites underlain by low permeability soils have been poor good candidates for in situ treatment

Hydraulic fracturing is a method of creating permeable sand lenses in the subsurface to enhance delivery or recovery of fluids from low permeability formations Several hydraulic fractures can be created from a single borehole with as little as 0 3 m of vertical spacing between them Typically, the fractures are circular to elongate in plan, have diameters of 9 to 12 meters, and contain 225 to 635 kg of coarse-grained sand

This report describes the results of pilot-scale soil vapor extraction (SVE) and bioremediation studies that were conducted at contaminated and uncontaminated sites to study the effect of hydraulic fractures on subsurface fluid flow through fine-grained soils The remedial technologies at the contaminated sites targeted hydrocarbons that leaked from underground storage tanks (USTs) Comparisons were made between the performance of wells containing hydraulic fractures and conventional wells Parameters of interest included well discharge, suction head distribution, and contaminant mass removal rates for the SVE wells, and infiltration rates, soil moisture contents, bioactivity, head distribution, and contaminant degradation rates for the bioremediation wells

## 1.2 Method

Hydraulic fracturing is a technique that is commonly used to increase the yields of oil and gas wells It has been adapted for use in the shallow subsurface to increase flow through fine-grained formations Hydraulic fractures are created when a fluid is injected into a borehole until a critical pressure is reached and the enveloping soil fractures With continued pumping, the fracture propagates away from the borehole The direction of propagation is a function of the relationship between the vertical and horizontal components of stress in the surrounding soil Glacial tills often contain high residual lateral stress induced by the weight of the overriding glacier When the lateral component of stress exceeds the vertical component, the soils are termed overconsolidated Fractures created in overconsolidated soils propagate away from the borehole in a horizontal to subhorizontal plane This geometry is favorable when utilizing vertical wells for delivery or recovery in the subsurface

The fracturing fluid is a slurry composed of an aqueous solution of guar gum and coarse-grained sand In solution, guar gum forms short-chain polymers that produces a fluid with the consistency of vegetable oil During fracturing operations, a borate solution is metered into the guar gum and crosslinks the solution to form long-chain polymers, producing a viscous gel capable of holding sand in suspension An enzyme, termed breaker, is also added at this time The breaker returns the gel to its pre-crosslinked

viscosity in approximately 12 hours, allowing the guar gum fluid to flow from the fractures into the well for recovery The sand remains in the fractures and provides permeable channelways for delivery and recovery

Injection of the fracturing slurry is performed through a lance-like device composed of a steel casing and an inner rod tipped with hardened cutting surfaces A drive head on the other end of the lance secures the casing and rod together Individual segments of the rod and casing are 1 5 m long and are threaded together as required by borehole depth After the lance is driven to the desired depth, the rod and conical point are pulled out, leaving soil exposed at the bottom of the casing A high pressure (24 MPa) water jet is then inserted to the bottom of the casing and rotated, cutting a disc-shaped notch 10 to 20 cm in diameter This notch will form the nucleus of the fracture (Figure 1 1) A simple measuring device, built from a steel tape extending the length of a tube and making a right angle bend at the end of the tube, is inserted to the bottom of the casing to verify and measure the radius of the slot

Subsequent to cutting the notch, an injection head outfitted with a pressure transducer is secured to the upper end of the casing to monitor the pressure during the fracturing operation The onset of pumping is marked by a sharp increase in pressure of the injection fluid followed by a marked decrease as the fracture propagates Sand is added to the guar gel after the pressure record indicates the onset of propagation The sand concentration is gradually increased until the ratio of the sand to gel (by volume) is in the range of 0 44 to 0 53 After one fracture is created, the rod is inserted into the lance and driven to a greater depth where another fracture is created

The major components of above-ground equipment are a slurry mixer, an injection pump, and gel mixing/storage tanks The slurry mixer is designed to continuously blend guar gum gel, the borate crosslinker, breaker, and sand It consists of a sand hopper, reservoirs containing breaker and crosslinker, a screw auger to introduce the sand to the gel, metering devices, and a mixing tube The guar gel is hydrated in 1900 liter tanks and pumped to the mixer The slurry exits the mixing tube and falls into the throat of a positive displacement pump, which injects it into the casing

Monitoring consists of a digital record of the pressure of the injection fluid and measurements of the deformation of the ground surface (uplift) during fracture propagation The injection pressure is measured by a transducer at the injection head and coupled to a data acquisition system, which displays the pressure log in real time (Figure 1 2) Uplift is measured at 25 to 35 stations in the vicinity of the borehole The measurements can be made with a leveling telescope or with a recently developed Ground Elevation Measurement System (GEMS) GEMS is a laser system that was developed to obtain uplift information in real-time during fracture propagation Uplift measurements are plotted on contour maps (Figure 1 3), and can be used to infer information about the size, thickness, and direction of propagation of the fracture The GEMS system provides a continuous display of uplift, which indicates propagation direction and safeguards against propagating fractures towards sensitive structures, such as retaining walls or building foundations

A more detailed description of the techniques used to create hydraulic fractures are described elsewhere (Murdoch and others, 1991a) The remainder of this report presents the details from each of the three study sites the Center Hill field site in Cincinnati, Ohio, the Xerox site in Oakbrook, Illinois, and the Dayton bioremediation site in Dayton, Ohio

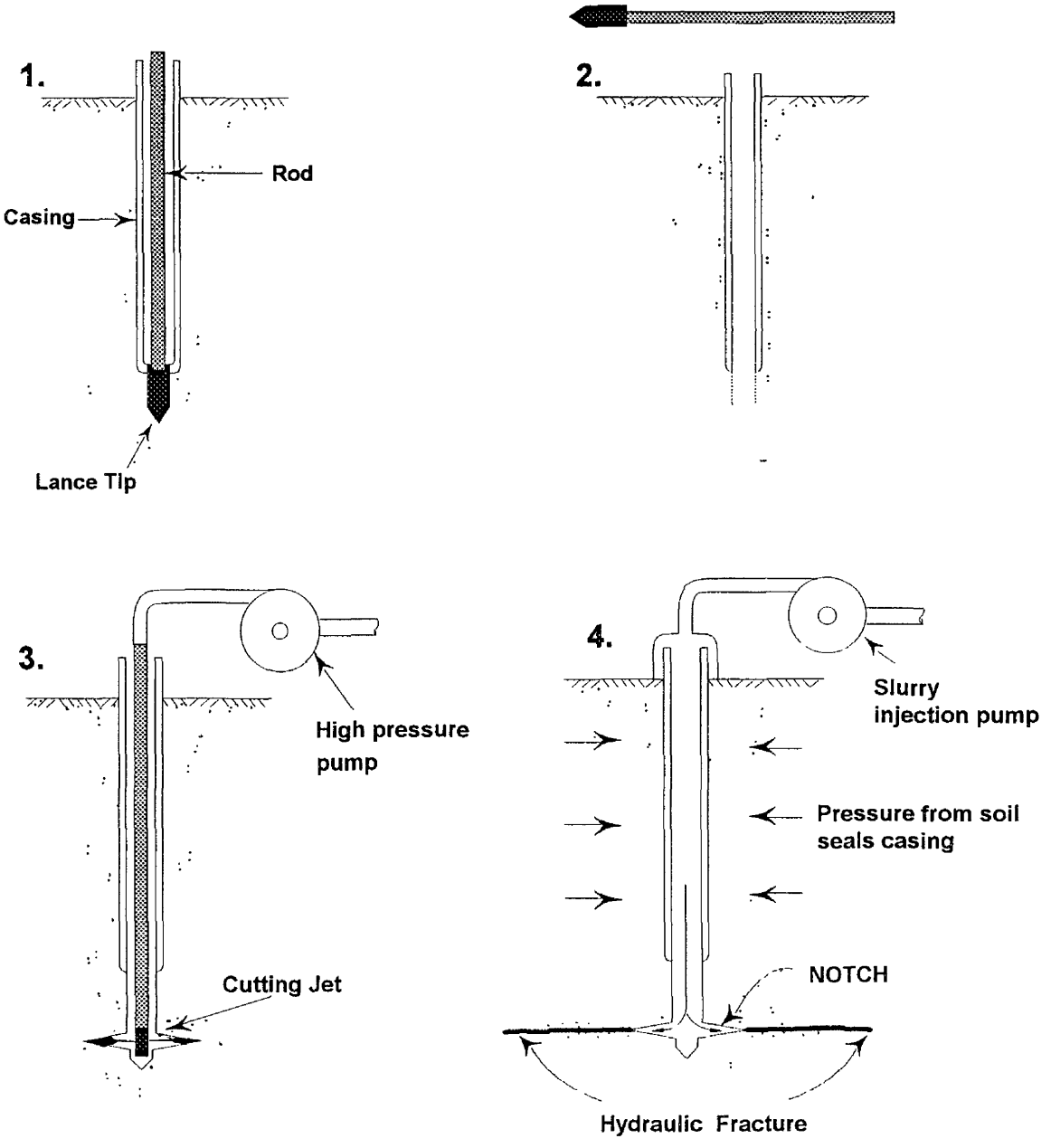


Figure 1 1 Method of creating hydraulic fractures

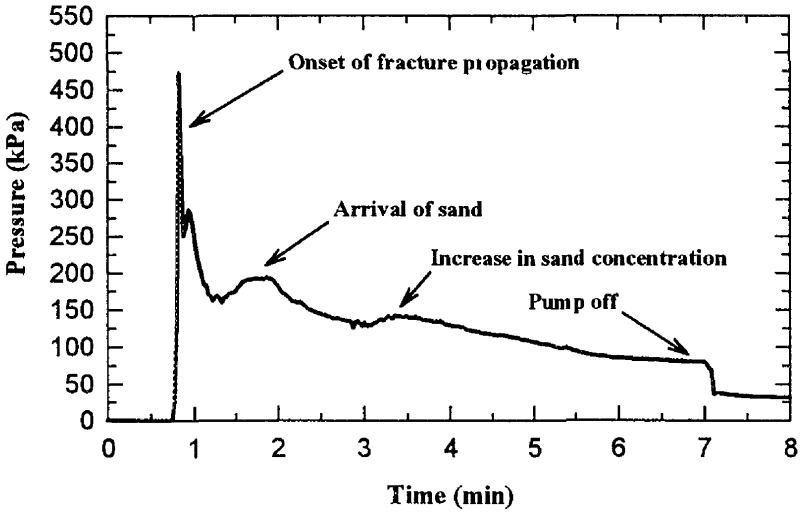


Figure 1 2 Log of injection pressure during hydraulic fracturing

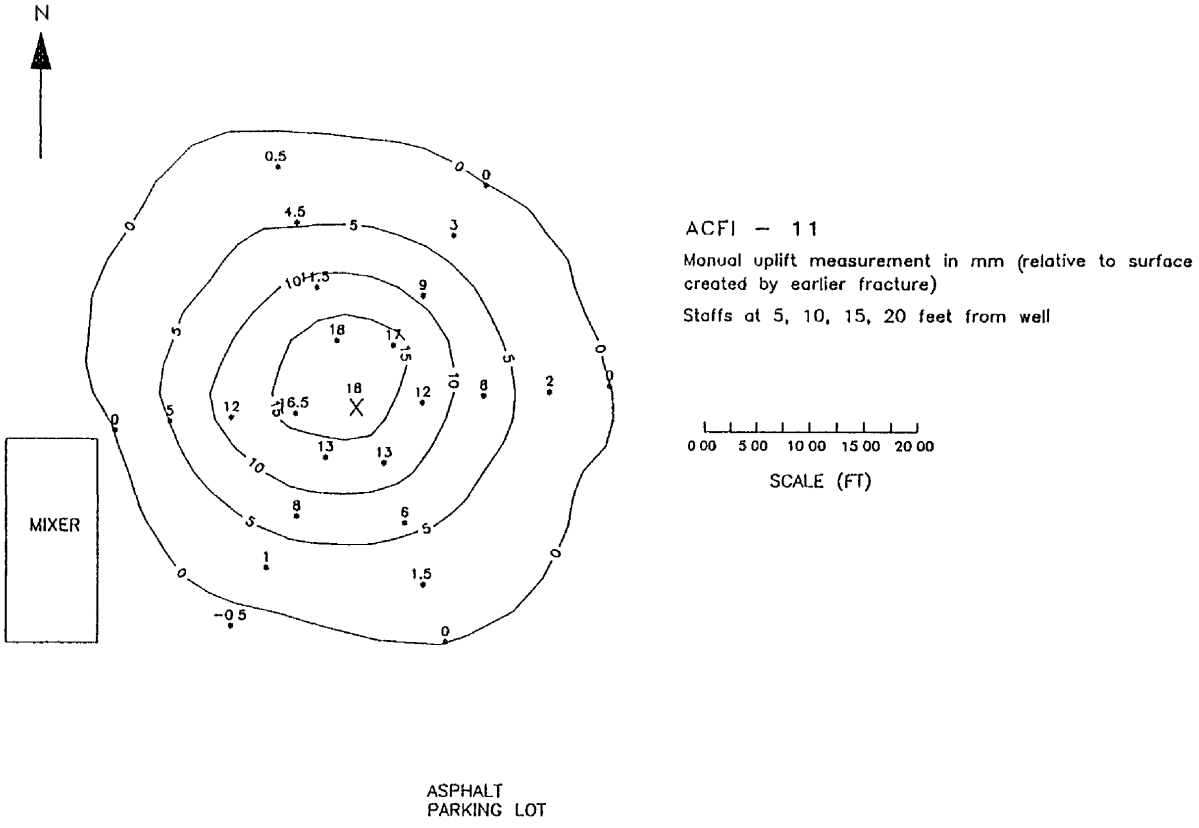


Figure 1 3 Contour map of surface displacement caused by hydraulic fracture

# 2.0 Center Hill Field Site

## 2.1 Objective

The effect of sand-filled hydraulic fractures on air flow in the subsurface was evaluated by comparing the performance of a well intersecting 3 hydraulic fractures and a conventional well that contained no fractures (Phase 1) A second study (Phase 2) was conducted to compare the performance of a well intersecting a single fracture, a well intersecting a single fracture that reached the ground surface (vented), and a conventional well that lacked fractures The ground in the vicinity of all the wells was pristine (there were no contaminants at the site), so both studies were limited to examining well discharge and subsurface pressure distribution in the vicinity of the wells

## 2.2 Site Characteristics

The studies were conducted at a site adjacent to the USEPA Center Hill Research Facility in Cincinnati, Ohio The site exhibits little relief and is underlain by glacial drift, which is predominantly silty clay with lesser amounts of sand and gravel Cobbles and larger clasts are common at depths greater than 3 m but are scarce at shallower depths The Phase 1 study area is overlain by several centimeters of coarse gravel and is used for parking Phase 2 was conducted in a field adjacent to the parking area and was covered with sparse vegetation

## 2.3 Experimental Design (Phase 1)

Two soil vapor extraction wells were used during Phase 1, a conventional well (CHC1) and a well intersecting 3 hydraulic fractures (CHF1) The wells were approximately 25 m apart Split-spoon exploration prior to the study indicated that the geology in the vicinity of both wells is similar

CHF1 intersected hydraulic fractures created at depths of 1 5, 3 1, and 4 6 meters (CHF1-5, CHF1-10, and CHF1-15, respectively) Subsequent to creating the fractures, split-spoons were driven to determine their spatial orientation The exploratory boreholes were then backfilled with non-shrink grout Typically, the fractures were shallowly dipping (10 to 15°), several millimeters thick, and extended 3 to 5 m from the borehole Details of the fractures are presented in Table 1 1

Each fracture at CHF1 was accessed by an individual 2-inch (nominal) PVC riser with a 45 7-cm-long wellscreen centered on the fracture The three risers were installed in the same 15-cm-diameter borehole Coarse-grained sand was used to fill the annulus between the borehole wall and the wellscreens, and non-shrink grout and bentonite were used to seal the areas between the screened sections and the top of the upper screen to the ground surface The conventional well (CHC1) was completed in an identical manner, with three separate risers and screened intervals at the same depths as CHF1

Pneumatic piezometers, constructed of 1/2-inch (nominal) PVC pipe, were installed in the vicinity of both wells Boreholes (5 cm in diameter) were created with a hand auger and the lower ends of the piezometers were buried in several centimeters of coarse-grained sand The remainder of the borehole was grouted to the surface with non-

shrink grout The upper end of each piezometer was outfitted with a quick-connect fitting that was matched to a digital manometer Piezometers were placed along radial lines extending from the wells at depths ranging from 108 to 128 cm

Table 2 1 Essential details of the fractures created for Phase 1

| Fracture I D | Depth (m) | Sand vol ($m^3$) | Slurry vol (L) | Max uplift (cm) | Size* (m) |
|---|---|---|---|---|---|
| CHF1-5 | 1 5 | 0 20 | 600 | 2 5 | 6 7 x 8 2 |
| CHF1-10 | 3 1 | 0 31 | 1184 | 2 2 | 6 1 x 8 2 |
| CHF1-15 | 4 6 | 0 26 | 1248 | 1 8 | 6 7 x 10 1 |

* inferred from uplift data and split spoon sampling

A one-horsepower blower, capable of producing 127 cm $H_2O$ suction, was installed at each well The three risers at each well were manifolded upstream of the blowers and outfitted with valves that allowed control of the suction on each riser In addition to the blower, each system included a water/vapor separator, variable-area flowmeters, piping, a vacuum-relief valve, and ports for measuring the pressure at various locations in the system

During equipment shakedown, the riser accessing the 4 6-m-deep fracture at CHF1 continuously produced water, necessitating frequent shut-downs of the SVE system to drain the water/vapor separator and pump the water from the well Consequently, suction was not applied to the lowermost screened sections (at both wells) during the study

Phase 1 was conducted over a 42 day period, from 20 January to 2 March 1992 Weather conditions during the period consisted of temperatures both above and below freezing, as well as several periods of rain and snow Well discharge and subsurface pressures at the pneumatic piezometers were measured 3 to 4 times per week The systems ran continuously, except when maintenance, such as draining the water/vapor separators or pumping water from the wells, was necessary Typically, both discharge and pressure reached steady values several minutes after the starting the blowers However, significant fluctuations occurred in both discharge and pressure following periods of precipitation, particularly at CHF1

## 2.4 Results (Phase 1)

Significant results of Phase 1 consist of well discharge and subsurface pressure distribution

### 2.4.1 Well Discharge

Vapor discharge from CHF1 ranged from 28 to 153 L/min and averaged 102 L/min In contrast, discharge from CHC1 was roughly an order of magnitude less, ranging from 8 L/min to 11 L/min, and averaging 9 3 L/min Discharge over the duration of the study is presented in figure 2 1 Fluctuations in discharge were common at CHF1, whereas the discharge at the conventional well remains relatively constant Typically,

decreases in discharge at CHF1 followed precipitation events, and subsequent increases in discharge followed the removal of water that had accumulated in the well For example, discharge for the first three days of the test is roughly 142 L/min It rained steadily on day 4, and vapor discharge gradually decreased over the next 12 days to 71 L/min By day 15, the well-screens at CHF1 were partially submerged in water Subsequent to evacuating the water, the vapor discharge increased from 71 to 113 L/min This pattern was repeated with a marked decrease in discharge following a particularly heavy rain on day 26 After this rain, water completely submerged the screened sections of CHF1, removal of the water again restored the discharge to the values before the rain

The discharge of CHC1 appeared to be independent of weather conditions, discharge varied only slightly during the study, and the well did not produce water

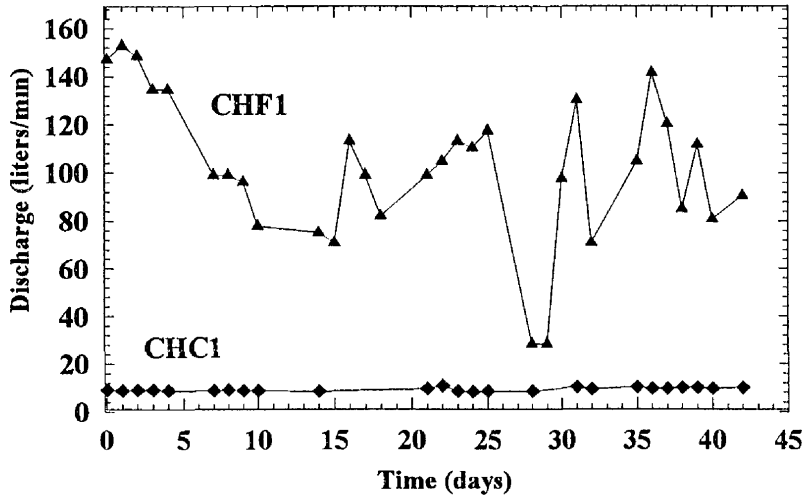


Figure 2 1 Vapor discharge as a function of time for wells CHF1 and CHC1

### 2.4.2 Pressure Distribution

Suction head was measured at the piezometer arrays installed around the perimeters of both wells several times a week throughout the duration of Phase 1 The suction head at each piezometer varied slightly throughout the test, typically demonstrating small increases following precipitation events, but the general distribution of suction head was roughly constant Figure 2 2 presents suction head as a function of radial distance from the wells The distribution of suction head is presented from a day when the suction head was greatest to highlight the maximum effect of each well

Suction heads in the vicinity of the fractured well are several times to roughly an order of magnitude greater than those at similar locations around the conventional well For the purpose of comparing the fractured and conventional wells, we used a suction head of 2 5 cm of water as a reference point to define a radial distance over which the well exhibits pneumatic control (this value is typically used by consultants to define the *radius of influence* of a SVE well)

The reference radius for CHF1 ranges from 6 1 m to greater than 9 1 m The pneumatic piezometer farthest from CHF1 was at a distance of 9 1 m, so effects greater than this distance from the well could not be measured On days when the suction head was greatest, this piezometer measured 6 9 cm of water Similar suctions were observed in the vicinity of the conventional well CHC1 at radius of approximately 0 3 m

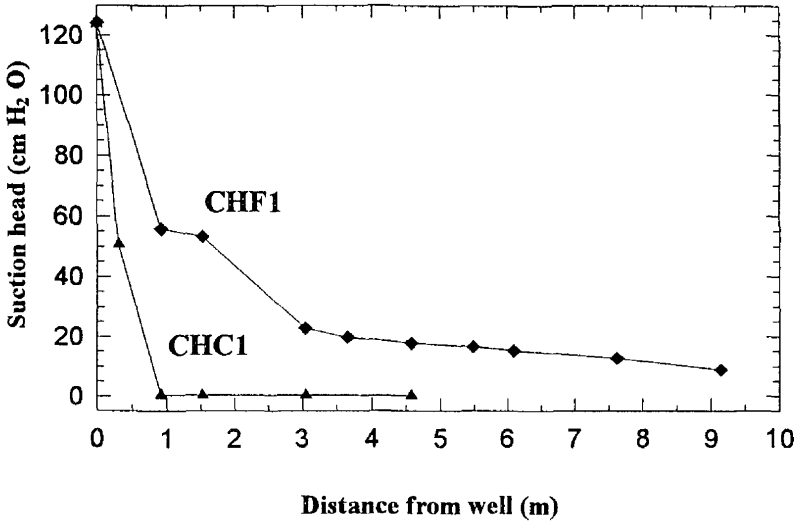


Figure 2 2 Suction head as a function of radial distance from CHF1 and CHC1

## 2.5 Experimental Design (Phase 2)

Phase 2 compared the performance of three wells, CHF2 and CHF3 intersected single fractures created at depths of 1 5 meters, and CHC2 contained no fractures The fracture created at CHF2 was allowed to vent to the surface (fractures typically climb towards the ground surface at a shallow angle and intersect the surface if a sufficient volume of slurry is pumped) Details of the fractures are presented in Table 2 2

The well completions for Phase 2 differed from those used during Phase 1 Wells CHF2 and CHF3 were constructed of 2-inch (nominal) PVC casing with a 15 2 cm screened interval centered on each fracture The casing was driven into the ground following the creation of the fractures, so that the slotted portion of the casing was in contact with sand in the fracture Accordingly, the casing was in contact with silty clay above and below the fracture, and the sand pack that was used in the Phase 1 completions was absent from CHF2 and CHF3 This completion method requires significantly less effort than methods involving drilling and sand packing

The well completions were designed primarily for vapor extraction, but inasmuch as water flowing into the wells markedly influenced vapor extraction during Phase 1, the completions were also designed to remove liquid They consist of a casing and screen that resembles a conventional completion, however, a 1 7-cm I D tube passes through a seal in the well head and extends to the bottom of the well Vacuum is applied to the tube

Opening a valve connected to the annulus between the tube and the casing sends a surge of air down the annulus and entrains any water that may have accumulated in the well

Table 2 2 Essential details of fractures created for Phase 2

| Fracture I D | Depth (m) | Sand vol ($m^3$) | Slurry vol (L) | Max uplift (cm) | Size* (m) |
|---|---|---|---|---|---|
| CHF2-F5 | 1 52 | 0 26 | 493 | 1 8 | 6 7 x 10 0 |
| CHF3-F5 | 1 52 | 0 14 | 312 | 1 7 | 7 9 x 7 9 |

*inferred from uplift and split spoon data

The SVE systems used during Phase 2 were the same as those used during Phase 1 The wells were manifolded upstream of the blower to allow control of the suction on each well, although once the system was operating, the suction applied to the wells was kept equal and was nearly constant Phase 2 was conducted over a 30 day period from 8 June to 7 July 1992 Moderate to warm temperatures and several rainfall events characterized the summer tests

## 2.6 Results (Phase 2)

Significant results of Phase 2 consist of well discharge and subsurface pressure distribution

### 2.6.1 Well Discharge

During Phase 2, discharge from the fractured wells exceeded that from the conventional well by an order of magnitude or more Discharge from the well intersecting the fracture that vented, CHF2, ranged from 173 to 204 L/min and averaged 190 L/min, whereas discharge from the fracture that did not intersect the ground surface, CHF3, ranged from 76 L/min to 116 L/min and averaged 105 L/min In contrast, discharge from CHC2 ranged from 4 L/min to 35 L/min and averaged 17 L/min (Figure 2 3)

Discharge was effected by weather conditions in a similar manner to Phase 1 The discharges from the fractured wells decreased briefly following heavy rains on days 10 and 26 Even the discharge from conventional well CHC2 was apparently affected by a particularly intense rainfall on day 10, decreasing from 19 to 8 L/min, although the discharge was unaffected by the rainfall on day 26

The well intersecting the fracture that vented, CHF2, provided a greater discharge than the other wells, but it is more sensitive to rainfall For example, the discharge at CHF2 decreased from 201 to 190 L/min following rainfall of 0 5 cm on day 8 (Figure 2 4), but the discharges of the other wells increased slighty during that time Apparently, the proximity of the fracture to the ground surface increases the amount of infiltration that temporarily diminishes vapor flow

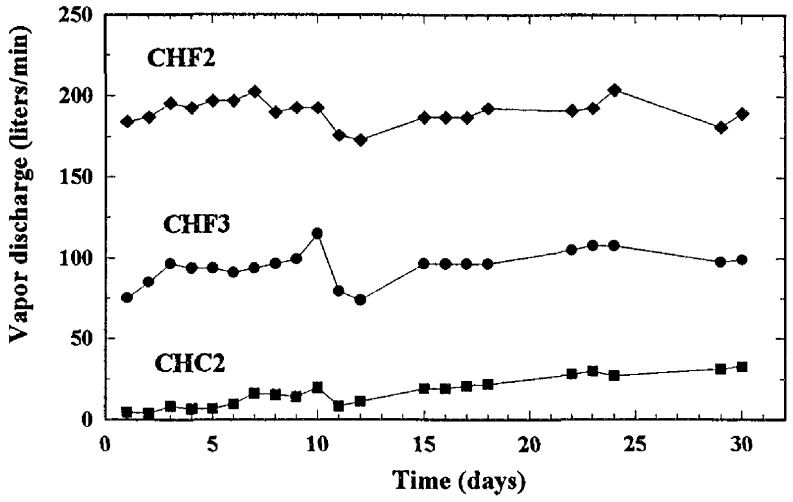


Figure 2 3 Vapor discharge as a function of time for wells CHF2, CHF3, and CHC2

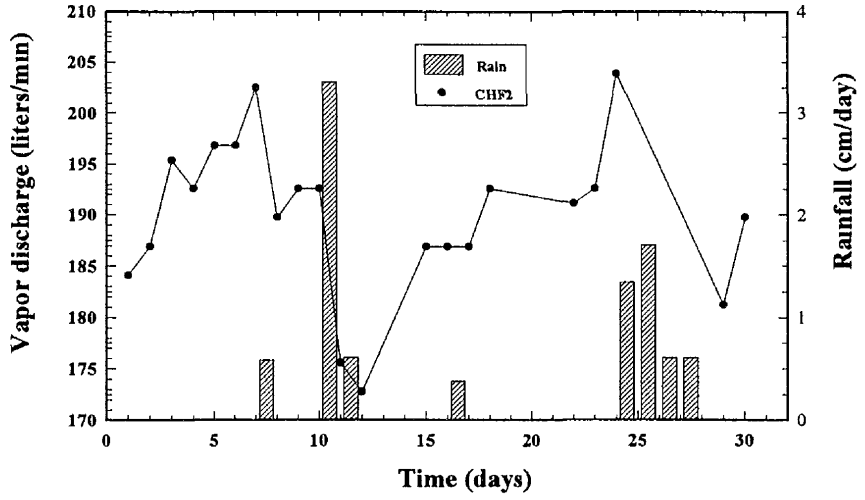


Figure 2 4 CHF2 discharge and rainfall as a function of time

Phase 2 was designed to include one fracture, CHF2, that vented (7 m from the well), and another, CHF3, that remained below the surface Both fractures were created at the same depth (1 5 m) and had similar dips (10 to 12°), however, CHF2 contained approximately twice the volume of CHF3 (0 26 $m^3$ and 0 14 $m^3$ of sand, respectively) The average discharge of CHF2 was 190 L/min, whereas that of CHF3 was 105 L/min These data suggest that as much as 45 percent of the air discharge from CHF2 may enter the fracture where it intersects the ground surface However, this estimate is an upper

limit of the effect of the vent because some of the increase in discharge certainly results from the difference in size Moreover, the southern half of CHF3 was located beneath a layer of loose top soil that became saturated after rainfall As a result, water contents beneath the southern half of CHF3 were greater than elsewhere on the site Suctions at piezometers to the south of CHF3 were consistently less than to the north Both the site conditions and the size would have contributed to the differences between CHF2 and CHF3 As a result, the effect of a hydraulic fracture reaching the ground surface may be significantly less than indicated by the data presented here

### 2.6.2 Pressure Distribution

The distribution of pressure in the vicinity of CHF2 and CHF3 are different from that of CHF1 (Figures 2 5 and 2 6) Suction head decreases between well CHF2 and the piezometers at radial distances of 0 9 to 1 5 m, but then it increases with increasing distance and reaches a maximum 3 to 4 6 m from the well The suction head then decreases at greater distances The distribution of pressure appears to be related to the location of the hydraulic fractures relative to the piezometers The hydraulic fracture CHF2-F5 climbs toward the ground surface, so that the most proximal piezometers overlay the fracture, the piezometer at 3 m radius intersects the fracture, and the piezometers at greater distances underlie the fracture (Figure 2 7) The location of the fracture clearly affects the magnitude of suction head measured at a piezometer It is noteworthy, however, that the reference radius (measured at 0 9 m depth) of both fractures is greater than 6 1 m

The fracture CHF2 is asymmetric with respect to the well, with the major axis of propagation to the northwest, and the suction head induced by the fracture mirrors this asymmetry Significant suction heads occur to the northwest of the well, but suction head decreases rapidly to the southeast These data underscore the importance of monitoring the propagation and determining the location of the fracture at depth, because the details of the fracture location will control the distribution of pressure in the subsurface

Clusters of piezometers were installed in the vicinities of CHF2 and CHF3 to evaluate the distribution of suction head as a function of depth The most meaningful data were obtained from a cluster 3 m west of CHF2, where five piezometers were installed at depths from 0 7 m to below the fracture Data from that cluster show that suction head decreases with distance normal to the fracture (Figure 2 8) Two piezometers, at 1 1 and 1 m are screened in the fracture, and show a suction head of 33 (cm of water), whereas the one 0 1 m above the fracture shows a suction head of 32 5 (cm of water) Suction head 25 4 cm above the fracture is 21 8 (cm of water), whereas 25.4 cm below the fracture it is slightly less, approximately 17 8 (cm of water)

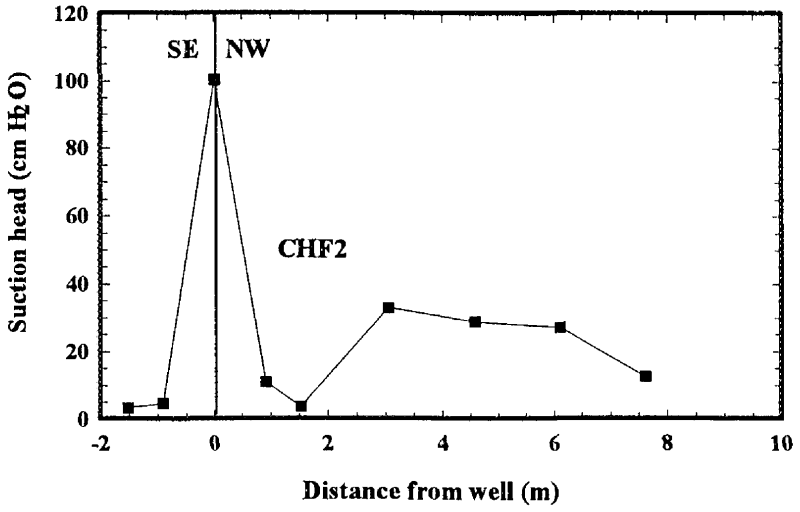


Figure 2 5 Suction head as a function of distance from well CHF2

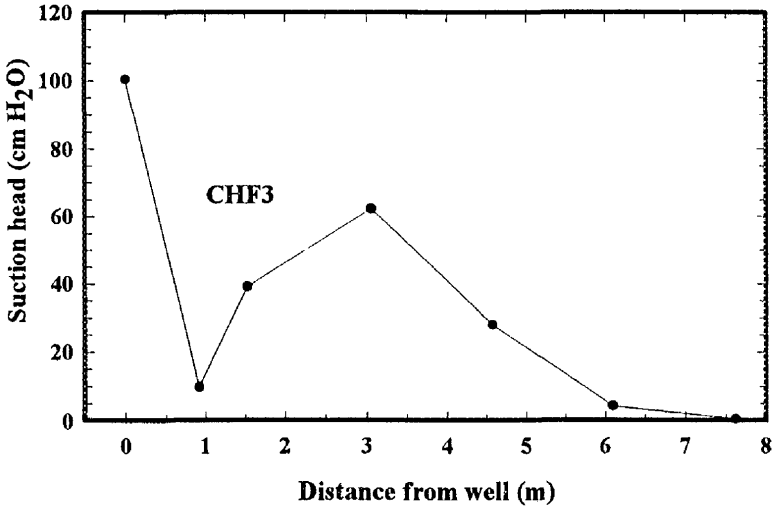


Figure 2 6 Suction head as a function of distance from well CHF3

The data indicate that vertical pressure head gradients are present above the hydraulic fracture that vented Thus, air flow vertically downward through the soil toward the fracture at a radial distance of 3 m is inferred even though the fracture is able to draw air directly from the ground surface 7 m from the well The vertical head gradient is approximately 0 5 and the estimated permeability of the till was $9 \times 10^{-9}$ cm$^2$ This corresponds to a downward flux of about 0 3 m$^3$/m$^2$ hr through the till overlying the fracture Assuming the plan area of CHF3 is approximately 30 m$^2$ indicates that the vertical flux 3 m from the well is approximately equal to the average flux This suggests

that most of the air produced from CHF2 may have flowed through the soil and that a small fraction entered where the fracture reached the ground surface

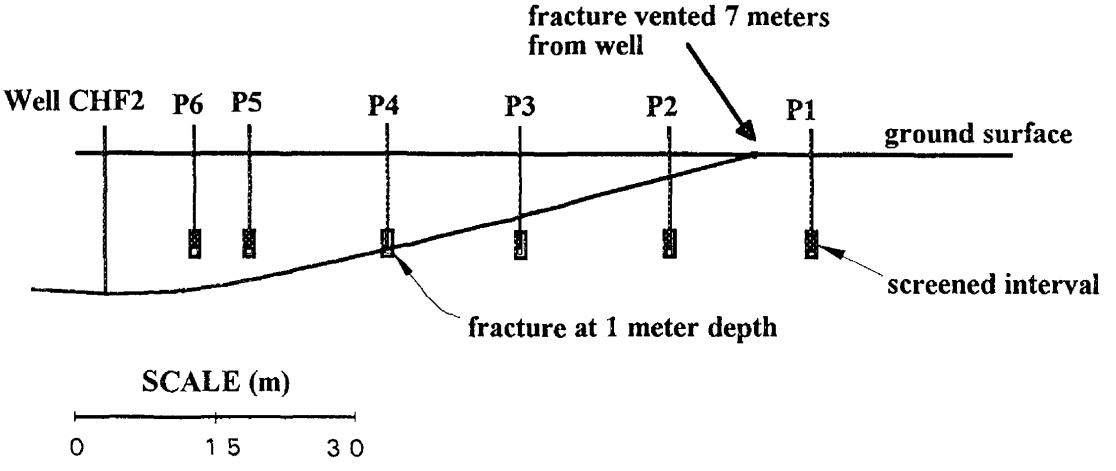


Figure 2 7 Cross section of fracture CHF2-F5 with pneumatic piezometer locations and screened intervals

Like well discharge, the pressure in the soil changed after rainfall Suction heads typically increased abruptly after rainfall and then decreased as the soil dried The response of piezometer CHF2-P4 (Figure 2 8) is representative of many of the piezometers Suction head decreased during dry conditions from the beginning of Phase 2 to day 6 when 0 58 cm of rain fell on the site Suction head increased from 19 1 to 21 2 cm of water during one day following the rain, but it continued to decrease until a heavy rainfall of 3 3 cm occurred on day 9 Suction head increased markedly, from 18 6 to 33 cm of water, following the rain, but it subsequently decreased to values similar to those before any rainfall

Similar changes occurred in the vertical distribution of pressure in the vicinity of CHF2 (Figure 2 8) Suction head increased approximately 12 7 (cm of water), although the distribution of suction resembled that from before rainfall Rainfall increases the moisture content and decreases the pneumatic conductivity of the upper few centimeters of the silty clay soil at the study site Apparently this reduces the air flow into the ground and diminishes discharge of the wells Moreover, decreasing the conductivity only at the ground surface increases suction head and changes the pattern of flow The decrease in well discharge following rainfall suggests that covering the site to prevent rainfall infiltration may be beneficial to remedial efforts at contaminated sites

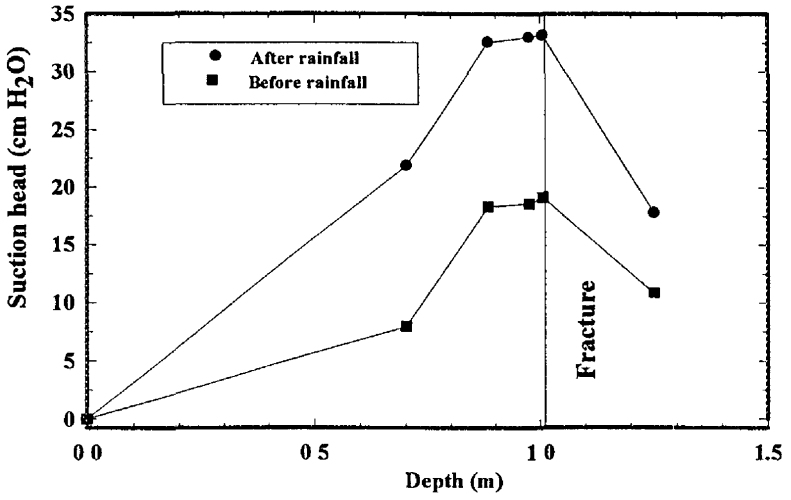


Figure 2 8 Effect of rainfall on suction head as a function of depth for a pneumatic piezometer 3 m from well CHF2

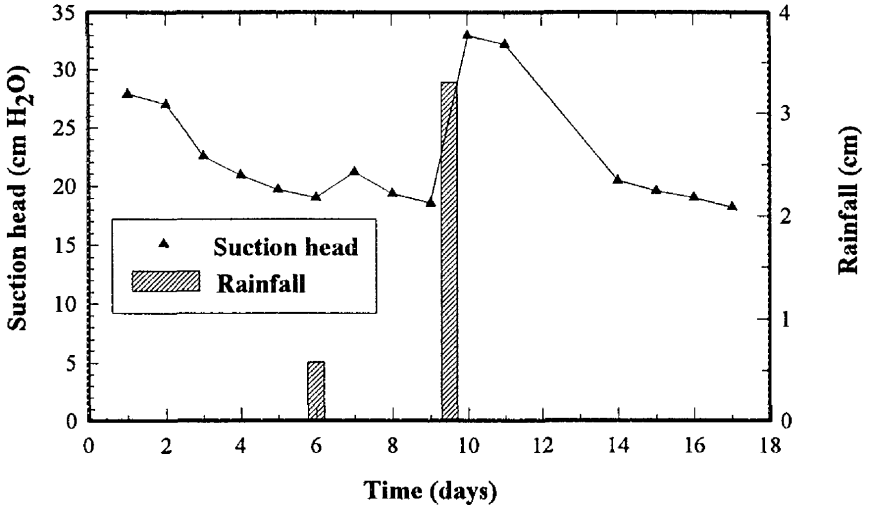


Figure 2 9 Suction head and rainfall as a function of time for a pneumatic piezometer 3 meters from well CHF2

## 2.7 Summary

Creating sand-filled hydraulic fractures in the vicinity of vapor extraction wells markedly affected both the discharge and the area influenced by the well (Table 2 3) The average discharges of the wells intersecting fractures ranged from 96 to 190 L/min, whereas the average discharge of conventional wells was roughly an order of magnitude

less, from 9 to 17 L/min A reference radius for each well was determined by estimating the distance from the well where the suction head was 2 5 cm of water Those distances were typically greater than 6 m for the wells intersecting fractures and less than 0 3 m for conventional wells lacking hydraulic fractures Both Phase 1 and Phase 2 tests showed the effects of rainfall, but the magnitude of those effects was much greater during Phase 1 The discharge from CHF1 decreased 80 or more L/min following rainfalls of several millimeters, whereas the discharge at CHF3 decreased approximately 37 L/min following rainfalls in excess of 2 5 cm Some differences in response might be due to variations in the geometry between fractures at CHF1, CHF2 and CHF3, and variations in antecedent moisture contents

The differences in well completions used during Phase 1 and Phase 2 are probably largely responsible for the change in well discharge response The well completions used during Phase 1 were designed to produce vapor only and the wells had to be opened and a pump installed to remove water In contrast, the well completions used during Phase 2 allowed water to be continuously removed from the well As a result, the slots in the wellscreen became submerged following rainfall during Phase 1, whereas they were never submerged during Phase 2 On one hand, this indicates that the rate of recovery of water from fractured wells is greater than that from conventional wells, which never produced water On the other hand, it highlights the need for designing wells to continuously recover both liquid and vapor phases Such a well design was shown to reduce the detrimental effects of water accumulated in the well

Table 2 3 Summary of well discharge for Phase 1* and Phase 2

| Well I D | Max discharge (L/min) | Avg discharge (L/min) | Avg ref radius (m) |
|---|---|---|---|
| CHF1* | 172 6 | 104 7 | 7 6-9 1 |
| CHC1* | 10 8 | 9 3 | 0 15-0 31 |
| CHF2 | 203 8 | 189 6 | 6 1-7 6 |
| CHF3 | 114 6 | 96 2 | 4 6-6 1 |
| CHC2 | 35 4 | 16 7 | < 0 31 |

Vapor discharge from a fracture that reached the ground surface, CHF2, was greater than discharge from one that remained in the subsurface, CHF3 However, CHF3 was smaller than CHF2, and half of CHF3 was overlain by loose topsoil, which trapped rainwater and increased water contents compared to elsewhere on the site Those two factors alone could account for less discharge from CHF3 than CHF2, so the effects of venting may be less than indicated by the available data Measurements of pressure as a function of depth clearly indicate gradients that will induce flow through the soil toward the fracture at CHF2

The purpose of these tests has been to compare the performance of hydraulic fractures to that of conventional wells, but by no means have we sought to maximize the performance of either system The above-ground equipment included a blower that could

apply 127 cm of water suction at the well head, which is modest compared to what can be attained using readily available, more powerful, vacuum pumps We expect, therefore, that well discharge could be increased, relative to values measured here, by applying a greater suction at the well head The magnitude of the increase is unknown, but it could be important when hydraulic fractures are used with vapor extraction to increase the rate of recovery of contaminants in soils

# 3.0 Xerox PR&S Facility

## 3.1 Objective

Volatile organic solvents contaminated silty clay underlying the Xerox PR&S facility to a depth of 4 6 m Comparisons were made between the performance of wells intersecting hydraulic fractures and conventional wells, parameters for comparison included well discharge, reference radius, and contaminant mass removal rates Hydraulic fractures, recovery wells, and pneumatic piezometers were installed by researchers from the University of Cincinnati The SVE system and flow monitoring equipment was designed and installed under the direction of environmental engineers from the Xerox Corporation and Haley and Aldrich, Inc (H&A) System monitoring and sampling was performed by Woodward Clyde and Associates

Fracturing in the contaminated section of the site was performed in July, 1991 Fractures were created from each of two boreholes, which were subsequently completed as SVE recovery wells Pneumatic piezometers, designed to measure subsurface pressure, were also installed at this time Two additional recovery wells, containing no hydraulic fractures, served as controls

## 3.2 Site Characteristics

The Xerox PR &S building is located 24 km west of downtown Chicago in Oakbrook, Illinois The facility occupies 3 7 acres and lies on clayey glacial drift interbedded with lenticular sand deposits Prior to October, 1975, the PR&S facility was known as the Machine Conditioning Center and was used to clean and refurbish photocopying machines Spillage and leakage associated with the use of these solvents resulted in contamination of the PR&S property (Golder,1986) Contamination was discovered in the vicinity of underground storage tanks and under the floor of the building Analysis of 29 samples from the PR&S property found total volatile organic halogen concentrations ranging from 3,677 to 150,000 ug/kg (Dames and Moore, 1990)

## 3.3 Hydraulic Fractures

Three hydraulic fractures were created from two separate boreholes in the contaminated section of the site The fractures were termed OXP1F1 through F3 and OXP2F1 through F3 In general, flat-lying to gently dipping fractures were created with the exception of OXP1F1

OXP1F1 was created at a depth of 1 83 m and vented at the surface several meters from the borehole after approximately one minute of pumping Ground-surface displacement (uplift) of 1 to 3 mm was observed in the vicinity of the injection point prior to venting This indicates that initially the hydraulic fracture formed was horizontal (in our experience, vertical fractures do not produce uplift that can be detected using a leveling telescope) Relatively soft material was encountered to a depth of slightly more than 1 m Presumably, a horizontal fracture was initially created at OXP1F1, but that the thickness of virgin till over the fracture was insufficient to contain it (a hydraulic fracture is expected to be vertical in fill) Essential details of the fractures are summarized below

Table 3 1 Essential details of fractures at the Xerox site

| Frac ID | Depth (m) | Sand vol ($m^3$) | Gel vol (L) | Max p (mPa) | Final p (mPa) | Max up (mm) | Radius (m) |
|---|---|---|---|---|---|---|---|
| OXP1F1 | 1 83 | - | 76 | 0 15 | 0 14 | 3 | - |
| OXP1F2 | 3 05 | 0 34 | 492 | 0 26 | 0 06 | 20 | 3 96 |
| OXP1F3 | 4 57 | 0 37 | 568 | 0 38 | 0 23 | 24 | 4 88 |
| OXP2F1 | 1 91 | 0 17 | 379 | 0 17 | 0 06 | 26 | 3 51 |
| OXP2F2 | 3 05 | 0 34 | 530 | 0 31 | 0 07 | 19 | 3 96 |
| OXP2F3 | 4 57 | 0 40 | 568 | 0 50 | 0 24 | 30 | 4 72 |

The table shows the depth below the ground surface where the fracture was created, the bulk volume of sand pumped into the fracture, the volume of gel in the fracture, the maximum pressure at the point of injection, the pressure at the end of pumping, the maximum uplift (typically not at the point of injection), and the approximate radius of the uplifted area over the fracture

Creating the fractures produced broad domes, with maximum vertical displacements of 20 to 30 mm, over areas roughly 7 0 to 10 0 m in maximum dimension For flat-lying fractures that are broader than they are deep, the uplift of the ground surface will serve as an estimate of the fracture aperture at depth The apertures of most of the fractures described above, except OXP2F2, probably can be estimated using uplift Most of the domes are roughly equant in plan, although the point of maximum uplift is almost always at a point other than the point of injection As a result, the fractures appear to be asymmetric with respect to the points of injection

In most cases, the asymmetry is slight, with the point of maximum uplift within a 0 9 to 1 8 m from the point of injection At OXP2F2, however, the point of maximum uplift was 4 5 m away from the point of injection In that case, the fracture appears to be elongate, with a preferential direction of propagation toward the area that was excavated to remove a solvent storage tank We suspect that the propagation of the fracture was affected, perhaps by turning upward, as it grew into the excavated area The fracture did not vent, and drilling was inconclusive, so details of the form of OXP2F2 are unknown

### 3.4 Fracture Modeling

A theoretical model of the growth of an idealized hydraulic fracture was developed by investigators at the University of Cincinnati and applied to data generated during this study The model assumes that the hydraulic fracture is flat-lying and circular, and that it opens solely by elastic deformation during lifting of the overburden Thin-plate theory is used to determine the ground displacements, and as a result the aperture of the fracture is tacitly assumed to equal the uplift of the ground A propagation criterion based on linear

elastic fracture mechanics is used to ensure equilibrium propagation Pressure within the fracture is assumed to be uniform, and the sand slurry is assumed to have remained a constant and uniform concentration during flow within the fracture

The theoretical model described above is able to predict many of the key elements of the hydraulic fractures created during the field test, even though the model remains highly idealized The following is a table of results of the model and values observed in the field

Table 3 2 Comparison of predicted and observed fracture results

| Fracture ID | $R_{frx}$ (m) | $R_{sand}$ (m) | $Up_{max}$ (mm) | $Up_{mid}$ (mm) | E (mPa) | $K_{Ic}$ (kPa $cm^{1/2}$) | $p_{final}$ (kPa) |
|---|---|---|---|---|---|---|---|
| OXP1F2 | 5 7 | 4 5 | 20 | 11 | 10 | 600 | 49 6 |
| observed | 4 3 | | 20 | 10 | | | 20 7-48 3 |
| OXP1F3 | 5 70 | 4 5 | 23 | 13 | 10 | 1200 | 144 8 |
| observed | 5 2 | | 24 | 12 | | | 103 4-179 3 |
| OXP2F1 | 4 0 | 3 3 | 27 | 15 | 10 | 700 | 62 1 |
| observed | 3 7 | | 26 | 15 | | | 41 4-62 1 |
| OXP2F2 | 5 5 | 4 5 | 23 | 13 | 10 | 700 | 60 7 |
| observed | 4 6 | | 19 | 7 | | | 51 7-68 9 |
| OXP2F3 | 5 3 | 4 3 | 27 | 15 | 10 | 1680 | 213 7 |
| observed | 4 6 | | 30 | 13 | | | 137 9-220 6 |

The parameter $R_{frx}$ is the maximum radius of the fracture from the model and the maximum radial extent of uplift in the field, $R_{sand}$ is the maximum radius of sand predicted by the model (it is less than $R_{frx}$ because the tip of a fracture is too narrow for sand to enter) and there is no comparable field data, $Up_{max}$ and $Up_{mid}$ are the maximum displacement and the displacement at half the radius, respectively where displacement is fracture aperture in the model and uplift in the observations, E is elastic modulus from the model, $K_{Ic}$ is the fracture toughness from the model, which is based on the length of the starter slot and the pressure required to initiate fracturing, and $p_{final}$ is the fluid pressure at the end of pumping, the range in observed fluid pressure reflects oscillatory nature of the pressure logs

The model slightly overestimates the maximum extent of the fracture, based on the uplift measurements However, the maximum extent of observed uplift was bounded by $R_{frx}$ and $R_{sand}$ for most of the simulations In practice, the maximum extent of uplift was difficult to locate precisely (kriging-based interpolation was used on the plots) and the model appears to be an adequate predictor of the extent of uplift

The model predicts the maximum amount of uplift, and the uplift at half radius to within a few mm in most cases One of the poorest fits, OXP2F2, is a highly asymmetric fracture that departs from the assumptions of the model

An elastic modulus of 10 MPa was used for all the analyses This value was selected because it yielded the best results during preliminary simulations It is roughly the value of elastic modulus from triaxial compression tests

### 3.5 Well and Pneumatic Piezometer Installation

Subsequent to the installation of the fractures, the boreholes were completed as recovery wells RW3 and RW4 both contained fractures at depths of 1 8, 3 0, and 4 6 m, and were completed so that each fracture could be accessed individually Two-inch nominal-diameter PVC risers were tipped with 0 3 m sections of screen that were centered on each fracture The annulus between the screened section and the borehole wall was filled with coarse sand and sealed with bentonite and non-shrink grout to prevent vapor flow between the fractures RW1 was completed with a single riser and screened from 1 5 to 4 6 m, whereas RW2, although it contained no fractures, was completed in the same manner as the fractured wells Table 3 3 summarizes the well configurations

Pneumatic piezometers were installed various distances from the recovery wells at several depths Piezometers were constructed of 1/2-inch nominal-diameter PVC pipe and were installed in individual boreholes The downhole ends of the pipe were wrapped with a geotextile and enveloped in a layer of coarse-grained sand Bentonite and non-shrink grout were placed above the sand to seal the piezometer and prevent leakage to the surface A hand-held digital manometer was used to obtain the subsurface pressure through a quick-connect fitting on the upper end of the piezometers

### 3.6 SVE System

The SVE system was installed soon after the wells were completed The vacuum pump, liquid/vapor separator, cooling system, and various system monitors were installed inside the PR&S facility Two-inch nominal-diameter schedule 80 PVC pipe was used to connect the vacuum system to the wells RW2, RW3, and RW4 were outfitted with manifolds and valves to allow control of the suction on each of the three risers RW1, which contained only one riser, did not require a manifold Vortex shedding flowmeters, which were coupled to dataloggers, were installed on the suction line for each well

The vacuum system consisted of a Sutorbuilt 1400 water-sealed vacuum pump driven by a 40 horsepower electric motor The unit was capable of producing 810 cm H20 (59 7 cm Hg) suction with a maximum flow of 13,000 L/min Liquid removed by the separator was treated with granular activated carbon before discharge to the sewer system A second separator was installed on the discharge side of the pump to remove any remaining liquid before the vapor was discharged to the atmosphere Both vapor and water samples were analyzed weekly to ensure that discharges were within guidelines established by the Illinois EPA A schematic of the SVE system is attached (Figure 3 1)

Table 3 3 Summary of well configurations

| Well I D | Fractures intersected | Number of risers | Screened section(s) |
|---|---|---|---|
| RW1 | none | 1 | 1 52 to 4 57 m |
| RW2 | none | 3 | 1 67 to 1 98 m<br>2 89 to 3 20 m<br>4 42 to 4 73 m |
| RW3 | OXP2-F1<br>OXP2-F2<br>OXP2-F3 | 3 | 1 67 to 1 98 m<br>2 89 to 3 20 m<br>4 42 to 4 73 m |
| RW4 | OXP1-F1<br>OXP1-F2<br>OXP1-F3 | 3 | 1 67 to 1 98 m<br>2 89 to 3 20 m<br>4 42 to 4 73 m |

System operating parameters such as inlet vacuum, seal water temperature, back pressure, total flow, and volume of liquid discharged were measured three times weekly In addition, wellhead vacuum, well discharge, subsurface pressure, and meteorological conditions such as air temperature, relative humidity, barometric pressure, and incidents of precipitation were recorded Vapor and water samples were obtained and analyzed either on site with a portable gas chromatograph or sent to an independent laboratory

### 3.7 Initial System Operation

The SVE system went on line in October, 1991 Initial vapor discharge was minimal as the site was dewatered Cold weather hampered early operation when water froze in the suction pipes and manifolds, requiring shutdown of the system until the outdoor plumbing could be heat-taped and insulated Due to the large volume of water being recovered, Xerox engineers designed a wellhead to remove water more efficiently The wellhead contains a valve that can be opened to allow ambient air into the riser The suction from the SVE system is applied to a 1 7 cm ID tube that runs down the center of the riser to the bottom of the well When the valve is opened to the atmosphere, air rushes down the annulus between the tube and the riser This surge of air entrains the water that has accumulated in the well and carries it to the liquid/vapor separator

Tests performed (March 1992) on the Xerox wells indicated that flow and subsurface pressure data received from the site did not accurately reflect actual conditions Flow data from the site, obtained from vortex-shedding flowmeters, reported negligible discharge from both the fractured and control wells However, measurements obtained with variable area flowmeters revealed significantly higher discharges than the vortex-shedding flowmeters registered For example, discharge from the 1 8-m-deep fracture at RW3 measured 481 L/min on the variable-area flowmeter but registered less than 28 L/min with the vortex-shedding meter In addition, discharge from the 3-m-deep fracture at RW3 measured 99 L/min whereas the vortex-shedding meter registered less than 28

L/min After consultation with the manufacturer, it was determined that the vortex-shedding meters could not accurately measure two-phase flow H & A engineers subsequently installed liquid-vapor separators upstream of the vortex-shedding meters to remove the liquid phase Subsequent flow measurements were taken utilizing both meter types

In addition, subsurface pressure readings obtained from the piezometers indicated minimal suction head in the vicinity of the wells During the well tests, however, it was discovered that many of the piezometers contained water It is suspected that water used to hydrate the bentonite seals saturated the gravel pack and the soil enveloping the piezometers This water remained trapped in the pore space and limited the ability of the soil to transmit pressure Consequently, new piezometers were installed in the vicinities of RW3 and RW2 without the excess water, the bentonite seals were hydrated by absorbing water from the non-shrink grout placed above them Subsurface pressure readings at the new piezometers increased dramatically, particularly in the vicinity of RW3 (Figure 3 2) New piezometers were installed in the vicinities of RW4 and RW1 several weeks later

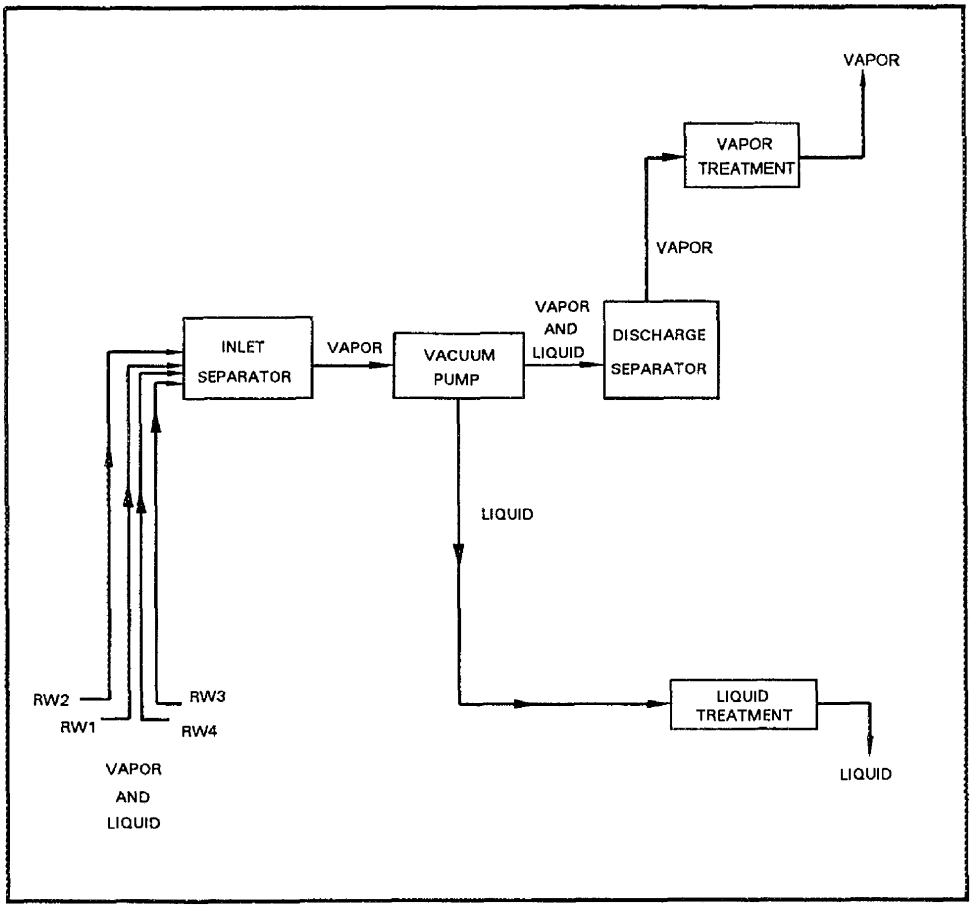


Figure 3 1 Schematic of soil vapor extraction system

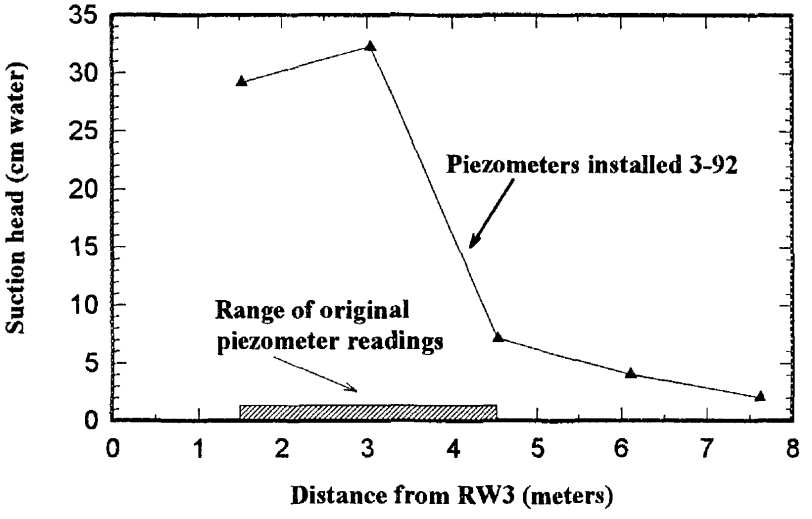


Figure 3 2 Subsurface pressure in the vicinity of RW3 after the installation of new piezometers (March 1992)

## 3.8 Results

The results present data collected 2 to 3 times per week during 158 days from June to November, 1992 The 158 day period marks the time when reliable contaminant concentration, well discharge, and subsurface pressure data was obtained Field data was obtained by personnel of Woodward Clyde and Associates and was forwarded to the University of Cincinnati and H&A for reduction and reporting Vapor analysis was performed on-site with a portable GC, duplicate samples were occasionally sent to an independent laboratory for confirmation of the results

### 3.8.1 Well Discharge

Well discharge data are presented in Figure 3 3 The data were obtained from a variable-area flowmeter placed in the vacuum lines at the wellhead manifolds, allowing measurements to be made on each riser A demister pot was utilized to remove liquid from the airstream before it entered the meter, minimizing the effect of two-phase flow on the accuracy of the readings Data from RW1 are omitted It was determined that a leak existed in the annulus between the riser and the borehole wall, allowing air from the surface to flow into the well Efforts to repair the leak were unsuccessful, so limited data were obtained from this well Table 3 4 summarizes the well discharge data obtained during this period

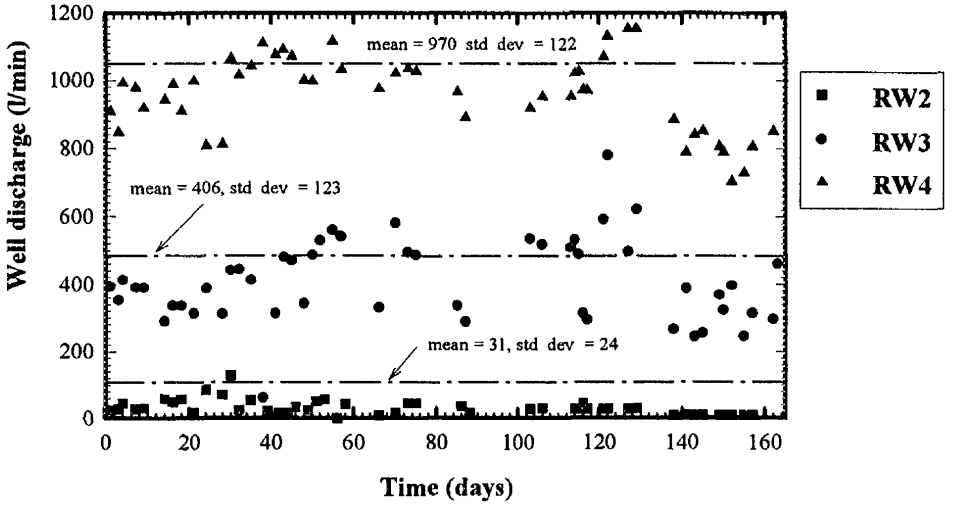


Figure 3 3 Well discharge with time Dashed lines represent average discharge

Table 3 4 Summary of well discharge for RW2, RW3, and RW4

| Well ID | Discharge range (L/min) | Avg discharge (L/min) | Discharge % 1 8 m zone | Discharge % 3 0 m zone | Discharge % 4 6 m zone |
|---|---|---|---|---|---|
| RW2 | 2 8-130 2 | 31 1 | 46 3 | 27 3 | 23 2 |
| RW3 | 62 3-623 0 | 404 9 | 61 2 | 8 4 | 30 4 |
| RW4[x] | 790 0-1209 1[x] | 968 4[x] | 36 0[x] | 41 0[x] | 23 0[x] |
| RW4[y] | 484 2-841 0[y] | 639 9[y] | - | not available | not available |

x-The 1 8-m-deep fracture at RW4 vented to the surface This data represents the discharge at RW4 when suction is applied to all three fractures y-Well discharge for RW4 when suction is applied to the 3 and 4 6 m-deep fractures only

The data indicate that discharge from the fractured wells is on the order of 15 to 20 times greater than from the unfractured well The discharge of the fractured wells tended to fluctuate whereas the conventional well discharge is consistently in a narrower range These fluctuations could result from changing soil moisture conditions caused by precipitation or from changes in the vacuum pump operation, but it is difficult to distinguish between the two effects when the data is in its present form

To separate the effects of subsurface conditions from variations in pump operation, the *specific discharge* was plotted as a function of time for the 1 8-m-deep fracture at

RW3 (Figure 3 4) The specific discharge is the ratio of the well discharge to the wellhead suction During a previous study at the Center Hill field site, it was determined that the specific discharge is unaffected by changes in suction at the wellhead (applying from 50 to 305 cm $H_2O$ suction) This is consistent with the theoretical analysis for air flow towards a well, which predicts a linear relationship between specific discharge and wellhead suction, and suggests that fluctuations in the specific discharge can be attributed to changing conditions in the subsurface

Figure 3 4 also presents the water recovery rates for the SVE system during the study The water recovery rate was obtained by dividing the total water discharged from the vacuum system during the period by the number of days in that period The shaded areas under the plots represent periods of relatively high and consistent water recovery, and are accompanied by relatively low specific discharge In contrast, during periods of decreased or sporadic water recovery, the specific discharge increases

The water recovery rate for the system and rainfall data from O'Hare Airport, which is approximately 16 kilometers north of the site, is presented in Figure 3 5 In general, and expectedly, peaks in the water recovery rate follow periods of heavy rainfall This is particularly clear on days 24, 86, 96, and 134 There are, however, periods when heavy rains are not followed by a substantial increase in the water recovery rate (days 10, 38, and 64) Factors that may effect the relationship between rainfall and water recovery are the intensity of the rainfall, which will effect infiltration and runoff rates, soil moisture contents at the time of the precipitation, and system downtime Also, rainfall data from the airport may not always reflect the amount of precipitation at the site In general, however, the relationship between rainfall, water recovery, and specific discharge indicate that infiltration of water into the subsurface decreases specific discharge Consequently, covering the site with an impermeable material may have been beneficial to remediation efforts

### 3.8.2 Contaminant Recovery

Contaminant recovery was evaluated by determining the concentrations of 10 target contaminants in the recovery stream, the mass rates of recovery, and the cumulative recovered masses at each well as functions of time The concentration data presented here is for the following compounds detected in the recovery stream dichloroethane, trichloroethane, ethylbenzene, perchloroethane, perchloroethene, trichloroethene, toluene, xylene, cis-1,2 dichloroethene, and trans-1,2 dichloroethene

Concentrations were scaled to a standard volume of air for convenience in Figure 3 7 In general, the concentrations ranged over more than an order of magnitude and were independent of the existence of hydraulic fractures for the particular conditions of this

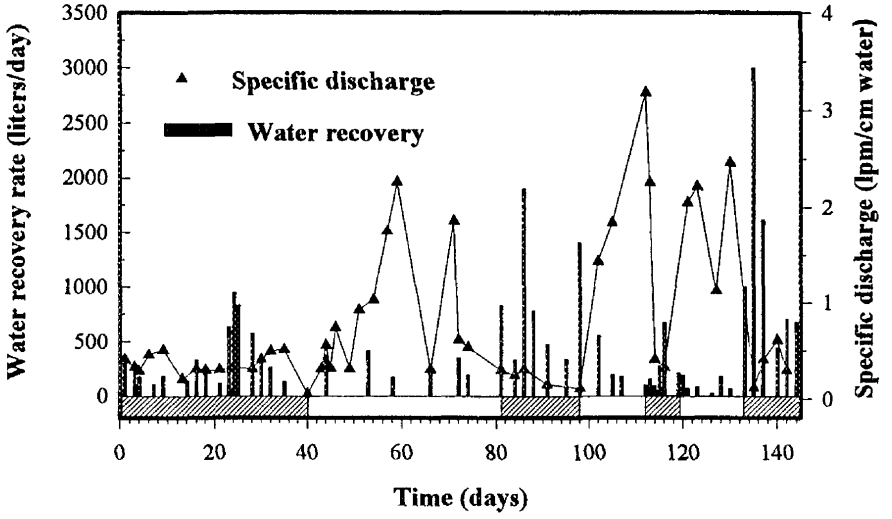


Figure 3 4 Specific discharge for the 1 6-m-deep fracture at RW3 and water recovery rate for the SVE system

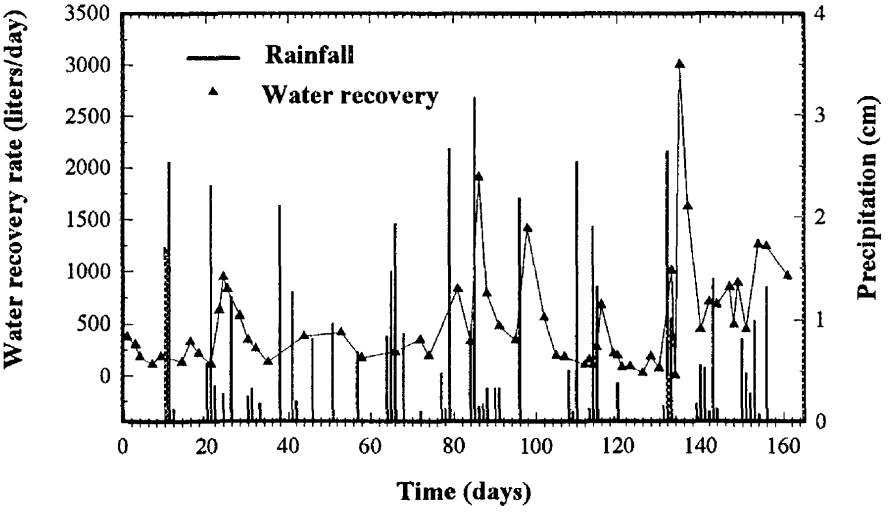


Figure 3 5 Water recovery for the SVE system and rainfall data

study For example, concentrations were consistently greatest from RW3, and they were consistently the least at RW4, with the control well RW2 providing intermediate concentrations The concentrations decreased with time throughout the duration of the

study Although there is considerable variation, the concentrations follow a simple power law

$$C = C_1 e^{-t/w} \quad (3\ 1)$$

where $C_1$ and $w$ are constants that amount to an initial concentration and a decay constant, respectively The decay constants for the three wells are remarkable similar, roughly 150 days, even though the concentrations themselves differ considerably (Table 3 4) The concentrations of contaminants from vapor extraction projects are known to typically decrease with time (USEPA 1991), and many follow the power law relation given above

A notable variation from the general relation describing concentration occurred between 3 and 19 August, when concentrations were unusually high The high concentrations were due to an increase in the recovery of perchloroethane (PCA), primarily from the 1 8 and 4 6-m-deep zone at RW2, the 3 0 and 4 6-m-deep fractures at RW3, and the 4 6-m-deep fracture at RW4 We investigated a variety of possible causes, including rainfall, applied suction, down time, and water recovery rate, but none of them can explain the high concentrations of PCA in early August

Table 3 5 Discharge, concentration, and mass recovery rates and coefficients

| Well | $Q$ (L/min) | | $C$ | | $m_r$ | |
|---|---|---|---|---|---|---|
| | Avg | Std Dev | $C_1$ (gm/L) | $w$ (days) | $C_1$(gm/min) | $w$ (days) |
| RW2 | 31 | 23 | $5\ 8 \times 10^{-4}$ | 154 | $4\ 7 \times 10^{-3}$ | 101 |
| RW3 | 406 | 123 | $12\ 4 \times 10^{-4}$ | 161 | $71\ 0 \times 10^{-3}$ | 142 |
| RW4 | 970 | 121 | $1\ 8 \times 10^{-4}$ | 175 | $35\ 0 \times 10^{-3}$ | 161 |

We conclude, therefore, that the processes that cause the concentration to change during vapor extraction appear to be unaffected by hydraulic fracturing The effect that hydraulic fracturing might have on the magnitude of the concentration, however, cannot be evaluated by these results In one case (RW3), the concentrations from the fractured well are consistently greater than from the control In another case (RW4), the concentrations from the fractured well are consistently less than the control In the latter case, however, the upper fracture reached the ground surface, so the effluent gas is diluted by air that never contacts contaminated soil

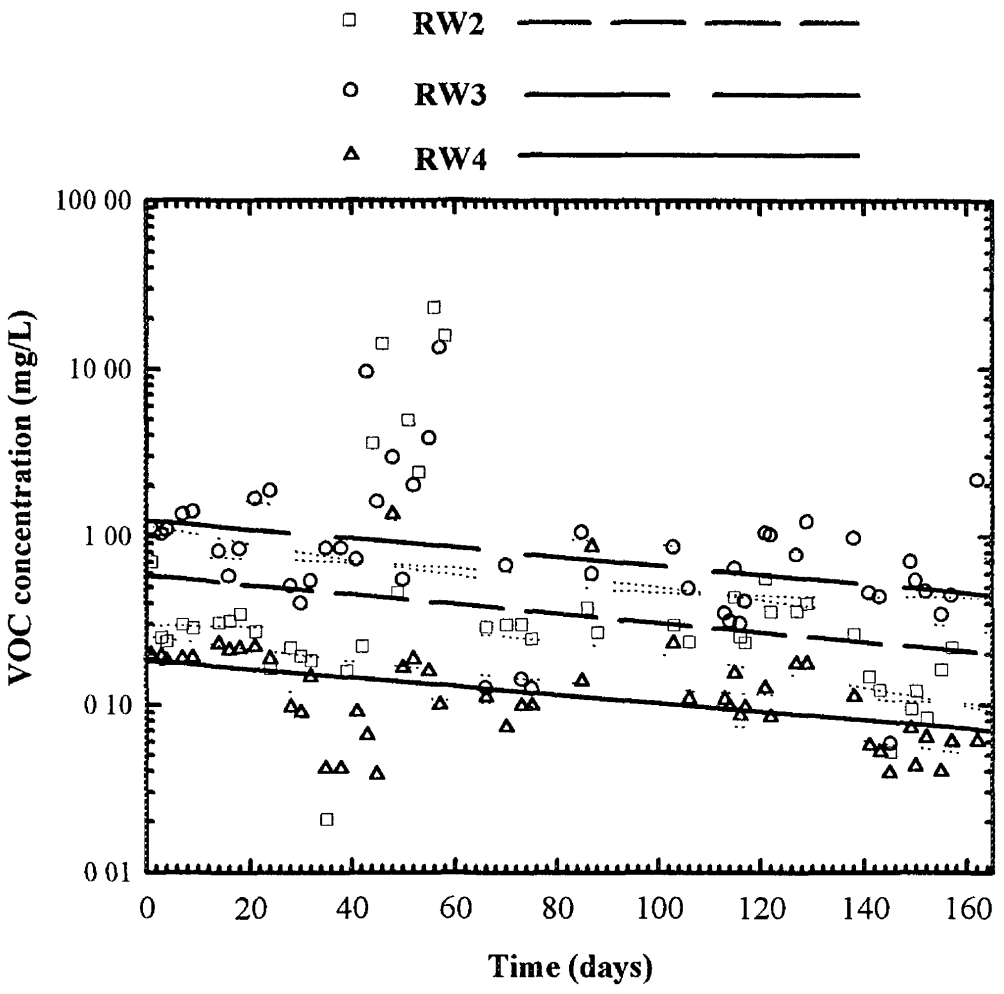


Figure 3 6 Combined concentration of 10 compounds recovered

### 3.8.3 Mass Recovery Rate

Mass recovery rate of each contaminant $m_{rp}$ was determined as follows

$$m_{rp} = C_2 C_p Q M_{wp} \qquad (3\ 2)$$

where $C_p$ is concentration of contaminant $p$ , $Q$ is volumetric discharge, and $M_{wp}$ is molecular weight of $p$, and $C_2$ is a constant to accommodate the proper units The mass rates for the ten target contaminants were then summed to give the total mass recovery rate Total rates were summed for each fracture to give the total rate for each well (Figure 3 7)

The mass recovery rates from the two hydraulically fractured wells are consistently one order of magnitude greater than that of the unfractured well Typically, the rates from all three wells decreases with time according to an expression that resembles equation (1)

Coefficients are given in Table 3 5 The coefficient $C_1$ characterizes the initial rates of recovery, and indicate an approximate order of magnitude difference between fractured and unfractured wells The decay constant $w$ of the control well is markedly less than those of the fractured wells, which are similar to the decay constants observed for concentration Accordingly, we infer that the recovery rate from the control well decreases faster than from both the fractured wells, although the recovery rates from all the wells show considerable variation throughout the duration of the study (Figure 3 7)

The relative rates of recovery of the two fractured wells is also noteworthy The rate of recovery from RW3, where all three fractures remained in the subsurface, was approximately twice the rate from RW4, where the upper fracture reached the ground surface Some of this difference certainly results from the lack of contaminants recovered from the upper fracture at RW4 as compared to RW3

### 3.8.4 Cumulative Mass Recovered

The mass recovery rate for each of the ten targeted contaminants was individually integrated to give the total cumulative mass of contaminant $M_{cp}$ as a function of time The cumulative mass recovered at time $t_m$ was obtained using

$$M_{cp}(t_m) = \sum_{n=1}^{m} m_{rp}\, \Delta t_n \qquad (3\ 3)$$

where a centered average based on the time of operation (the system was periodically inoperational due to a variety of factors) is used to determine the time increment

$$\Delta t_n = (t_{on+1} - t_{on-1})/2 \qquad (3\ 4)$$

with $t_{on}$ the operational time during measurement $n$ The cumulative mass yields were calculated to be 19 kg, 9 5 kg, and 2 7 kg, for RW3, RW4, and RW2, respectively, over the 158 day period (Figure 3 9) Much of the mass recovered from RW2 occurred during August, when concentrations were unusually high, whereas contaminants were recovered from the fractured wells throughout the study We expect that considerably more contaminants were recovered by vapor extraction at the Xerox site than indicated by those results

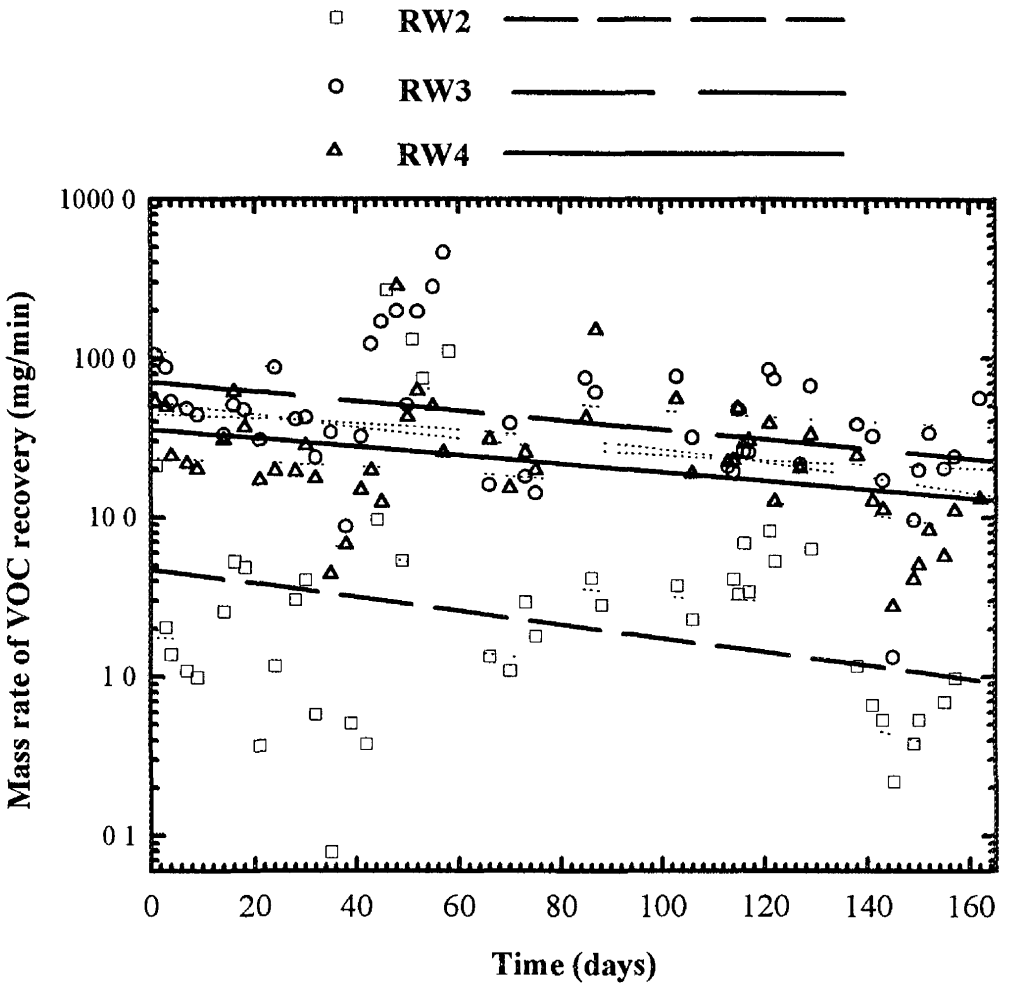


Figure 3 7 Mass recovery rates

In some cases, an unknown compound eluted during GC analysis just outside the retention time window for 1,1,1,-TCA This compound has not yet been identified, and is omitted from the calculations of the cumulative mass yield In addition, contaminants recovered during operation from November, 1991 to June, 1992 have been omitted from this estimate Discharge data obtained prior to June were from vortex-shedding flowmeters, which were unable to measure the discharge rate of the mixture of water and vapor that was typically recovered from the wells As a result, the volumetric discharge and mass recovery rates cannot be determined with the same confidence as the data presented here We expect, however, that the mass contaminant recovery rates before June may have been greater than they were after June Contaminant recovery rate decreased exponentially throughout the study period in a manner consistent with other vapor extraction operations It follows that the recovery rate was probably greater during the months preceding the study than it was during the study itself, and that volatile organic compounds may have been recovered that were omitted from routine chemical analyses

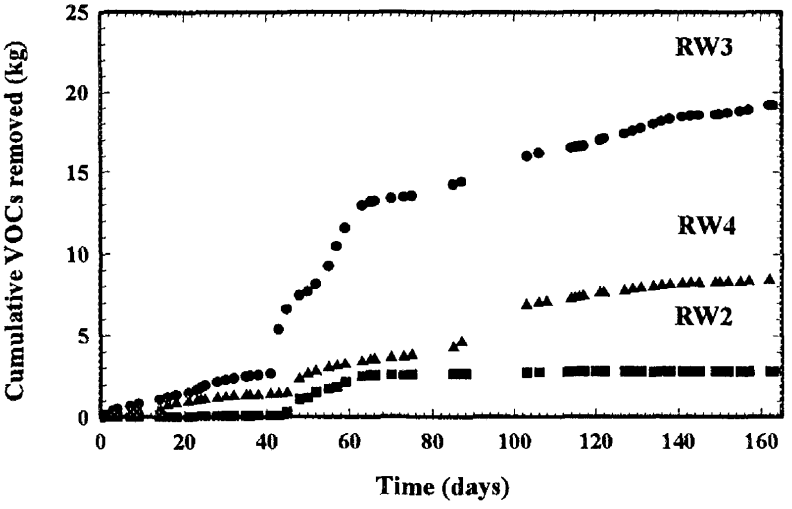


Figure 3 8 Cumulative mass recovered

### 3.8.5 Subsurface Pressure

Subsurface pressure readings were obtained from pneumatic piezometers every 2 to 3 days with a hand-held digital manometer with an accuracy of +/- 5 mm of $H_2O$ Suction at the wellheads and below the surface in the vicinity of the unfractured wells varied little over the duration of the study Suction head was consistently in the 620 to 725 cm of $H_2O$ range at the well and decreased to a few millimeters of $H_2O$ at piezometers 1 5 m from RW2 In contrast, soon after piezometers were installed in March, the distribution of suction head in the vicinity of the fractured well RW3 decreased gradually from 40 6 to 33 0 cm of $H_2O$ between radial distances of 1 5 and 3 0 m (at approximate depth of 1 5 m), it decreased abruptly from 33 0 to 7 6 cm over the next 1 5 m of radial distance, then decreased gradually at greater radial distances A suction head of 3 1 cm was observed at a 7 6 m radius The hydraulic fracture extended to approximately a 3 m radius, so suction head appears to be elevated in the vicinity of the fracture and to decrease markedly at the distal edge of the fracture It is noteworthy, however, that significant suction heads were observed at distances approximately two times the radial length of the fracture Similar distributions of suction head were observed around fractured wells in silty clay in Cincinnati, and are consistent with theoretical analyses of air flow in the vicinity of permeable lenses

The suction heads in the subsurface were by no means constant and those recorded soon after the piezometers were installed were among the highest observed at the Xerox site For example, suction head at 1 5 m radius decreased from 40 6 cm in March to between 5 1 and 7 6 cm at the beginning of the detailed study in June The suction head gradually increased, however, and was in the range of 12 7 to 17 8 cm at the end of the study Suction heads at the other piezometers also decreased between March and June, and then increased gradually during the period of detailed study

The cause of the changes in suction head in the subsurface with time is unclear, but it could be related to infiltration of rainwater During studies at Center Hill it has been observed that pneumatic piezometers may become isolated from the soil and fail to measure suction if they become wet, either from infiltration or from water used to hydrate bentonite seals Once they become wet, several weeks or more may be required before the piezometers function properly Presumably, water displaces air and prevents air flow in the vicinity of the piezometer It seems feasible that the measurements made in March characterize the distribution of suction head in the vicinity of the well, and that subsequent measurements underestimated the suction head because infiltrating water accumulated in the piezometers

The form of the distribution of suction head in the subsurface during the study period (Fig 3 9) resembles that observed in March, although the magnitudes of the suction are less Suction heads on the order of several millimeters are typically observed at radial distances of 7 6 m

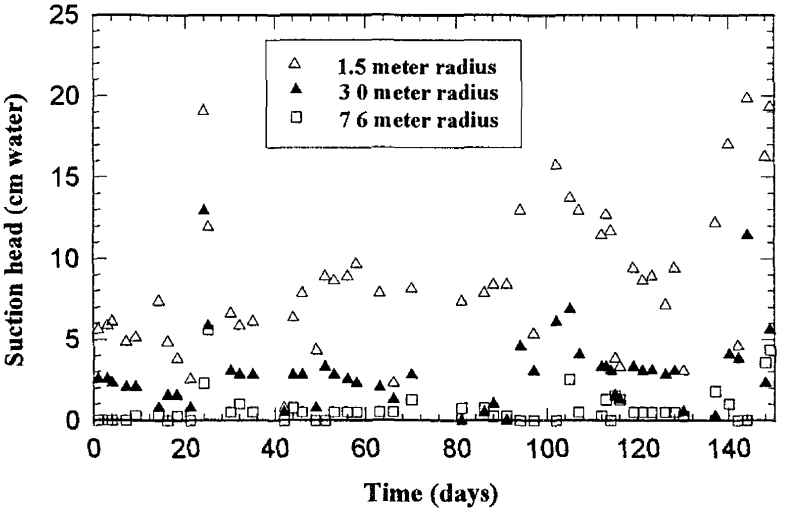


Figure 3 9 Suction head in the vicinity of RW3

Creating hydraulic fractures appears to have extended the distance where suction head is affected by a well from approximately a meter to more than 7 6 m at the Xerox site Translating the distribution of suction into a measure of the area affected during vapor extraction is problematic, however, because there is no generally recognized method of estimating that area. Some environmental consultants define a radius of influence of a vapor extraction well as the distance where a suction head of 0 25 or 2 5 cm of $H_2O$ can be measured in the subsurface Certainly the capability of a vapor extraction to effectively remediate an area will depend on applied pneumatic gradient, as well as the pneumatic conductivity and effective porosity of the soil, the Henry's Law coefficient of the contaminant, the time required for remediation, possible biological influences and other factors Accordingly, the use of suction head alone seems insufficient to estimate the area that will be remediated

### 3.9 Summary

The performance of one multi-level conventional well, RW2, was compared to the performance of two multi-level wells, RW3 and RW4, each containing hydraulic fractures nucleated at depths of 1 8, 3 0, and 4 6 m Most of fractures were shallowly dipping and were confined to the subsurface, except the 1 8-m-deep fracture at RW4 was steeply dipping and reached the ground surface All three wells were placed in areas of equivalent concentrations of contaminants, according to data obtained from soil samples prior to the test The wells were evaluated with tri-weekly measurements during 160 days of vapor extraction

1 Vapor discharge from the conventional well averaged 31 L/min, whereas it averaged 405 L/min from RW3 and 968 L/min from RW4 Some of the difference in discharge between RW3 and RW4 appears to be from air that is drawn in from the ground surface through the upper fracture of RW4 Hydraulic fractures appear to increase the vapor discharge by factors of 13 to more than 20

2 The concentration of volatile contaminants was approximately 2 times greater from the fractured well RW3 than from the conventional well RW2 Curiously, the concentration from RW4, the other fractured well, was roughly an order of magnitude less than from RW3 Much of that difference, however, is probably due to dilution of the recovered vapors by air that flows in through the upper fracture and never contacts contaminated ground

The concentration from all of the wells decreases with time as a negative exponential The decay constants from the three wells are roughly similar, although the decay in concentration from RW2 is slightly more rapid than from the fractured wells

3 The mass recovery rate from fractured wells was 7 to 14 times greater than from the conventional well on average throughout the 160-day-long test Mass recovery rate also decreased according to a negative exponential The decay constant for the conventional well is approximately 70 percent shorter for the fractured well

4 Suction was essentially undetectable within a meter of the conventional well, whereas suction was commonly detected 7 6 m from the fractured well RW3 Suction measured at piezometers was greatest soon after the piezometers were installed, and decreased markedly over the few months between installation and the period of study However, suctions generally increased throughout the duration of the 158-day-long study

5 This report presents data obtained during a 158 day period from June to November, 1992 Prior to this time, discharge data was obtained from vortex-shedding flowmeters, which were unable to accurately measure two-phase flow Therefore, volumetric discharge and mass recovery rates during this period cannot be determined with confidence During the 158 days of this study, concentration and mass recovery rates decreased exponentially, suggesting that concentrations and mass recovery rates during the period prior to June were greater than those during the period of this study Therefore the cumulative mass of contaminants recovered from the site exceeds the values presented in this report

6 Several problems were encountered during the operation of the vacuum, monitoring, and chemical analysis systems These conditions were remedied prior to collection of the data presented in this report These include a) overheating of the vacuum pump due to exhaust system failure b) process piping and sample tube freezing c) flow monitoring equipment malfunctions d) failure of the on-site gas chromatograph e) system fouling due to the accumulation of solids from evaporating cooling water

# 4.0 Dayton Bioremediation Site

Bioremediation exploits the capacity of microorganisms to transform organic matter into innocuous byproducts and is currently being utilized for the in situ remediation of organic contaminants The rate of biodegradation, however, can be limited by a lack of subsurface nutrients (oxygen, nitrogen, or phosphorous), available moisture, unfavorable pH or temperature, and various characteristics of the indigenous microbial population (Atlas, R M and D Pramer, 1990, Leahy, J H and R R Colewell, 1990) It has been demonstrated that delivering supplemental nutrients and oxygen to the subsurface can enhance in situ bioremediation (Ryan et al, 1991), however, the capacity to deliver and disperse nutrients is often limited in soils of low permeability Consequently, low permeability soils have been poor candidates for in situ bioremediation

## 4.1 Objective

The objective of this study was to determine if hydraulic fractures could be utilized to enhance the delivery and dispersion of aqueous nutrients and oxygen in fine-grained soil The performance of a nutrient injection well containing hydraulic fractures and a conventional injection well were compared Parameters for comparison included, injection rate, well pressure head, pressure head distribution, soil moisture content, and bioactivity in the vicinities of the wells

## 4.2 Site Description

The site is a former fuel distribution and storage facility in Dayton, Ohio Leaking underground storage tanks (USTs) contaminated the underlying silty clay glacial drift to a depth of 3 7 m The site is currently inactive, all USTs, associated plumbing, and structures have been removed It occupies approximately one acre and is covered with sparse vegetation and gravel This study targeted an area of undisturbed soil adjacent to the tank removal area

## 4.3 Hydraulic Fractures

The hydraulic fractures were created from a single borehole at depths of 2 2, 2 4, 3 1, and 3 7 meters (July 1991) Ground surface deformation measurements were made during the fracturing operations using a leveling telescope Creating the fractures produced broad domes, with maximum vertical displacements of 12 to 23 mm, over areas roughly 9 to 14 meters in dimension Most of the domes were equant to slightly elongate in plan, although the point of maximum uplift was usually at a point other than the point of injection As a result the fractures appear to be asymmetric with respect to their points of injection

The spatial orientation of the fractures was determined by split-spoon sampling subsequent to creating the fractures (all exploratory boreholes were filled with nonshrink grout after sampling was completed) In general, the fractures dip toward the parent borehole at dips of 28° to 30° The uppermost fracture intersected the ground surface (vented) approximately 3 7 m north of the parent borehole (the vent was expected to have negligible effect on the study results)

Essential details of the fractures are summarized in Table 4 1, which gives the depth at the point the fracture was created, the bulk volume of sand injected, the volume of gel injected, the maximum pressure at the point of injection, the pressure at the end of pumping, the maximum uplift (typically not at the point of injection), and the approximate radius of the uplifted area over the fracture

Table 4 1 Essential details of the hydraulic fractures

| Frac ID | Depth (m) | Sand vol ($m^3$) | Gel vol (L) | Max p (kPa) | Final p (kPa) | Max up (mm) | Radius (m) |
|---|---|---|---|---|---|---|---|
| SAD2-A | 2 2 | 0 17 | 416 | 289 6 | 48 3-75 8 | 22 | 4 6 |
| SAD2-B | 2 4 | 0 17 | 379 | 117 2 | 48 3-103 4 | 20 | 4 5 |
| SAD2-C | 3 1 | 0 26 | 416 | 255 1 | 68 9-137 9 | 17 | 5 0 |
| SAD2-D | 3 7 | 0 26 | 473 | 289 6 | 124 1-179 3 | 12 | 7 0 |

### 4.4 Well Installation and the Injection System

The borehole used to create the fractures was completed as an injection well (SAD2) with a 2-inch nominal diameter PVC riser and wellscreen The screened section, which was approximately 1 7 meters long, extended from slightly above the uppermost fracture to slightly below the lowermost fracture Coarse-grained sand was used to fill the annulus between the wellscreen and the borehole wall, and the area above the sandpack was grouted to the surface with non-shrink grout The conventional well (SAD4) was completed in the same manner

A system was installed (November, 1991) to deliver an aqueous solution of hydrogen peroxide (an oxygen source) and nutrients to the wells The system consisted of various automated metering pumps and control valves that mixed water, hydrogen peroxide, and a nutrient solution in the proper concentrations The system was contained in a trailer that was parked several meters higher in elevation than the wells, allowing the solution to flow by gravity from a holding tank to the wells A recovery trench, installed down hydraulic gradient of the test area, collected the injected water and prevented off-site migration The system was designed, installed, and operated by the Foppe-Thelen Group, Cincinnati, Ohio Details of the system are proprietary and have not been published

### 4.5 System Operation

The injection system went on line in December 1991 and was monitored for a period of 278 days Over the duration of the study, weather related and mechanical problems caused intermittent operation The study can be divided into three periods, defined by the regularity of flow to the wells (Table 4 2) System operation was intermittent from day 1 to 80 (Period I) due to freezing temperatures and associated mechanical problems Over the next 121 days (day 81 to 202), the system operated per

design (Period II) with occasional shutdowns of short duration Mechanical problems resulted in sporadic operation from days 202 to 278 (Period III)

Table 4 2 Periods of system operation

| Period | Description | Duration |
|---|---|---|
| I | Intermittent operation due to frozen pipes and other mechanical problems | Dec 6, 1991 to Feb 29, 1992 (days 1 through 80) |
| II | Regular operation with occasional shut downs of short duration | March 1 to June 30, 1992 (days 81 through 202) |
| III | System not operational a majority of the time due to mechanical problems | July 1 to Sept 14, 1992 (days 203 through 278) |

## 4.6 Sampling

Soil samples were obtained for testing and chemical analysis three times during the study period The first sampling episode, which provided baseline data, took place in September, 1991 (subsequent to creation of the fractures and prior to the onset of injection) The second sampling event occurred in February, 1992 (during Period I), and the third in July, 1992, (during Period III)

Split spoon samples were taken along a radial line extending from each well at distances of 1 5, 3 0, and 4 6 meters Continuous samples were obtained from a depth of 1 2 to 3 7 meters The sample cores were double-wrapped in plastic and zip-lock bags, and transported to the laboratory in iced coolers

Piezometers were installed in the boreholes created during the first round of sampling The piezometers were constructed of 3/4-inch nominal diameter PVC pipe and were enveloped in a sand pack and grouted to the surface with nonshrink grout Subsequent samples were obtained 30 cm east (February 1992) and 30 cm west (July 1992) of the piezometers All sampling boreholes were backfilled with nonshrink grout

## 4.7 Laboratory Analysis Procedures

The sample cores were cut into 2 5 cm sections that were analyzed sequentially for microbial population, moisture content, fluorescein diacetate hydrolysis activity (FDA), pH, and contaminant concentrations

### 4.7.1 Microbial Characterization

The upper 2 5 cm of each core was taken for total microbial number counts on an R2A medium and for specific contaminant degrader numbers by plating on SM medium (Vesper et al, 1993) This was done by aseptically shaving the outer layer from the section, then removing 1 g of soil and placing it in a 12 ml sterile tube with 5 ml of sterile water The soil plus water was then sonicated for 5 min at 90% power of a Heat Systems model W375 sonicator For total microbial numbers, the sonicate was plated on R2A medium using the Spiral Platter (Spiral Systems, Inc , Cincinnati, Ohio) The plates were

incubated at 29° C until the number of colonies on the plate could be counted (usually 48 hrs) For specific contaminant degrader numbers, the SM medium was amended with the plates placed in sealed dessicators containing a gasoline fume environment

### 4.7.2 Moisture Contents

The section of the core from 2 5 to 5 0 cm was taken for moisture content (weight water/weight of solids) analysis This section of soil was placed in a pre-weighed aluminum pan, then dried at 110° C until no further weight change was detected

### 4.7.3 FDA Analysis

The section of the core from 5 0 to 7 5 cm was taken for fluorescein diacetate (FDA) hydrolysis analysis (Schnurer, J and T Rosswall, 1985) The section was aseptically shaved to remove the outer layer Then one gram of the inner core was placed in a 125 ml sterile dilution bottle containing 100 ml of a 60 mm sodium phosphate buffer (pH 7 6) plus 0 5 ml of the stock FDA solution The stock FDA solution was made by adding 2 mg of FDA (Sigma Chemical Co ) per ml of acetone The contents of the bottles were mixed on a reciprocating shaker set at about 50 shakes per min The samples were incubated in a controlled temperature room at 12° C for 24 hrs After the incubation, samples were centrifuged at 13,000 rpms for 1 min The supernatant was monitored at 490 nm using a Perkin Elmer Spectrophotometer

### 4.7.4 BTE and TPH analysis

The cores were analyzed for benzene, toluene, and ethyl benzene (BTE fractions), and total petroleum hydrocarbons (TPH) The samples taken for BTE fractions were obtained by taking the lower 15 cm from each split spoon sample and placing it quickly into 300 ml of methanol in EPA type jars The samples were then tested as dictated in EPA Standard Method SW846 (USEPA, 1990) The total petroleum hydrocarbon samples were taken during the microbial analysis preparation As described above, core sections were shaved to remove the outer layer of soil After samples were taken for microbial analysis, the residuals from each core were combined and frozen at -50° C The TPH level for each sample was then determined using EPA Method 418 1 (USEPA, 1983)

## 4.8 Results

Well head pressure, injection rate, and head distribution in the vicinity of the wells was measured in the field to assess the performance of the wells Soil moisture content, microbial populations and their activity, and the concentration of contaminants in the vicinity of the wells were determined in the laboratory to gauge the effect of injecting the remedial fluids Each of these parameters is discussed in detail below

### 4.8.1 Well Pressure Heads

Well pressure head was monitored to ensure that differences in subsurface head distribution and injection rates at the two wells could not be attributed solely to differences in well head pressure With the exception of Period I, the pressure heads at the two wells were similar, although they fluctuated considerably (Figure 4 1) A majority of the fluctuation could be attributed to changes in the fluid level in the reservoir that supplied the wells, which periodically filled and drained between the limits of a float switch In general, increases (and decreases) in pressure head at SAD2 were accompanied by increases (and decreases) of similar magnitude at SAD4 In general, during Period II, the pressure head at SAD2 is moderately higher ($\approx$18 cm $H_2O$) than at SAD4, presumably because SAD2 was located at a slightly lower elevation

The wide disparity between the well pressure heads during Period I can be attributed to flow restrictors placed on the well heads during the early stages of Period I Initial injection rates exceeded expectations, so flow restrictors were installed at each well as a precautionary measure to ensure that hydraulic control of the site could be maintained The flow restrictor was removed from SAD4 after 8 days, whereas the restrictor at SAD2 was utilized throughout Period I After installation of the flow restrictor, the pressure head at SAD2 decreased abruptly to negative values (suction), indicating that the well's capacity to deliver fluid was underutilized Consequently, the flow restrictor was removed on day 81, which marks the onset of Period II

During Period II, the pressure heads fluctuated in the range of 101 to 193 cm of $H_2O$ at SAD2, and in the range of 112 to 165 cm of $H_2O$ at SAD4 During Period III, the pressure head data were limited because the system was inoperational a majority of the time

### 4.8.2 Subsurface Head Distribution

Heads in the vicinity of the wells were determined in one of two ways depending on the level of water in the piezometers When a piezometer was full of water, the head was measured with a pressure gauge that was matched to a fitting on the upper end of the piezometer If the piezometer was not full, head was determined by measuring the depth to water Datum was represented by the ground surface, so artesian conditions are indicated by positive head values

The head distribution shows considerable variation with time For example, heads varied markedly during 5 weeks in Period II at 4 locations in the vicinity of SAD2 and SAD4 (Figures 4 2 and 4 3) However, the magnitude of fluctuation appears to decrease with vertical distance from a fracture Heads over those 5 weeks vary by 127 to 152 cm of $H_2O$ at points intersecting fractures, whereas heads fluctuated by roughly half that amount at a piezometer screened 45 cm from a fracture Fluctuations of head in the vicinity of SAD4 were similar to those at points located away from fractures in the vicinity of SAD2

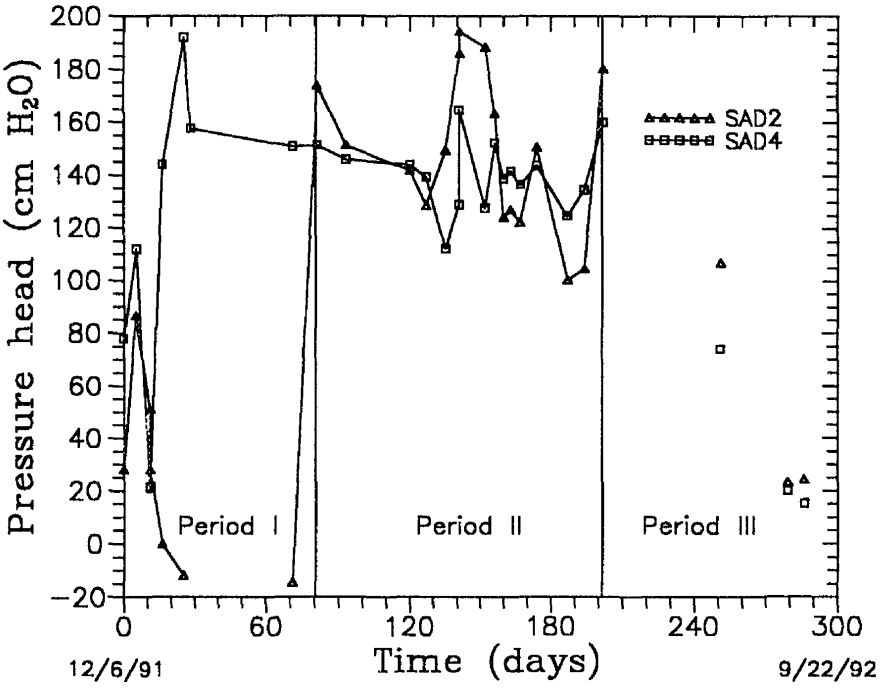


Figure 4 1 Well pressure heads

The subsurface head fluctuations appear to correlate with well head pressure fluctuations The decrease and subsequent increase in subsurface head in the vicinity of SAD2 and SAD4 from day 168 to 202 parallel the changes in well head pressure seen in figure 4 1

Heads at positions along fractures responded to changes in well pressure heads with time more dramatically than those at positions away from the fractures This resulted in relatively lower or higher head zones at points located away from fractures compared to those intersecting fractures

The spatial distribution of head varied with time, but we took heads from one day to represent the distribution during much of Period II (Figure 4 4) The plots are identified by the well I D , followed by the lateral distance from the well and the depth, respectively At that time, the heads in the vicinity of SAD2 increased with depth and decreased with distance from the well In addition, a band of relatively high head appears to occur at a depth of approximately 2 4 m Heads in the vicinity of SAD4 were always less than those observed near SAD2 The head distribution around SAD4 indicates that the head values at 1 7 m were typically higher than those at greater depths The overall distribution suggests flow away from SAD4 at locations 1 5 m from the well and downward flow at 1 7 m depth, 3 0 and 4 6 m away from the well

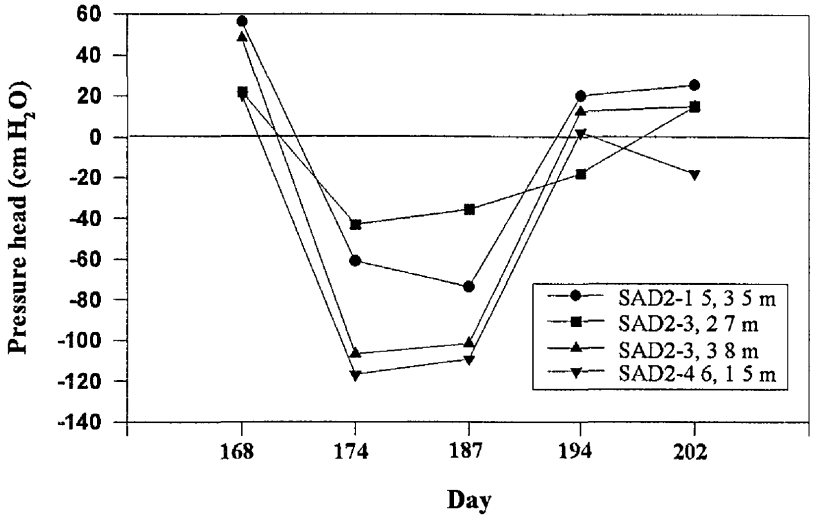


Figure 4 2 Subsurface pressure heads near SAD2

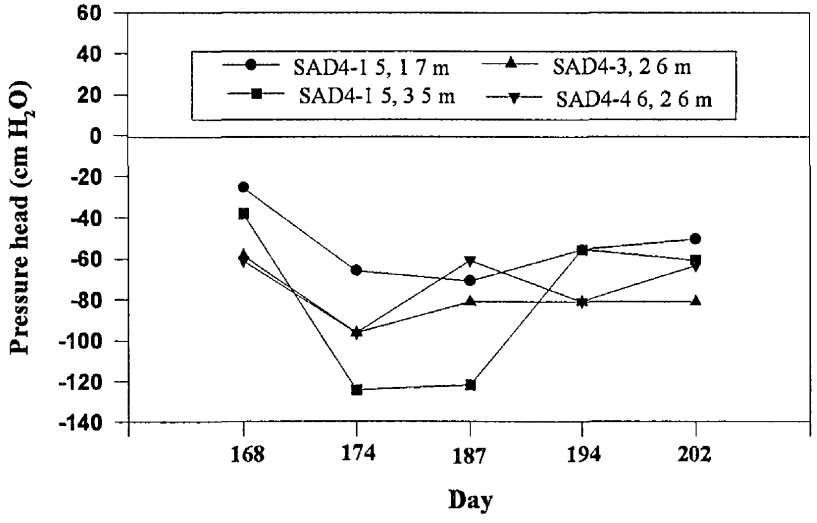


Figure 4 3 Subsurface pressure heads near SAD4

### 4.8.3 Injection Rates

Commercially available mechanical flowmeters capable of measuring small volumetric flow rates without significant head losses could not be located, and electronic flowmeters exceeded the budget limitations of this project, so a method of determining flowrates into the wells was developed Rates were determined by measuring the velocity of a dye injected into a 2 1-m-long transparent hose at the entrance of the well The time taken for the leading edge of the dye stream to travel the length of the hose was recorded, and the velocity of the dye was obtained The product of the velocity and the cross-

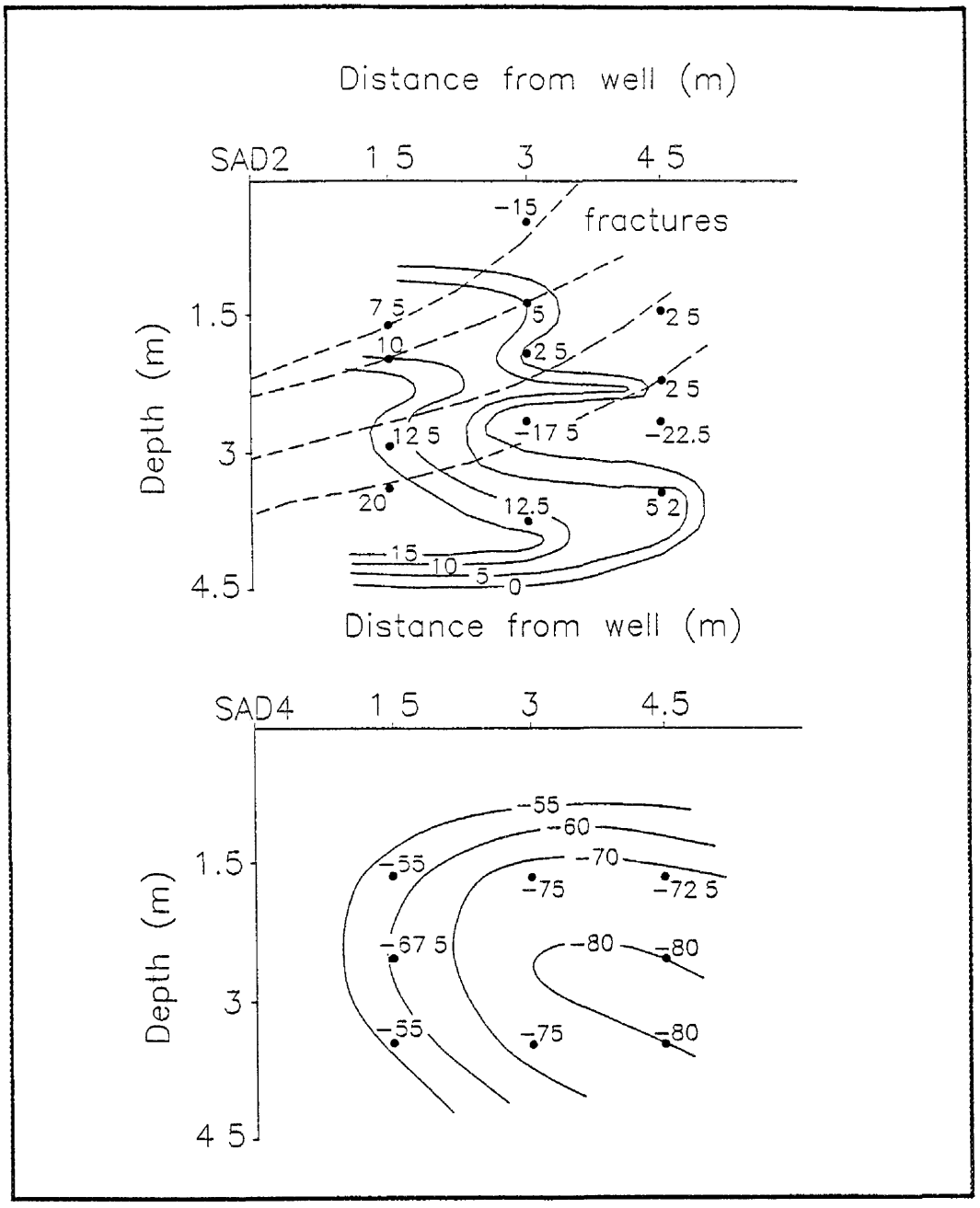


Figure 4 4 Comparison of subsurface pressure heads in the vicinities of SAD2 and SAD4

sectional area of the hose provided the flowrate Laboratory testing of this method, where rates could be controlled, indicated that it was reasonably accurate For the low flow rates seen at SAD4, however, errors in the measurement could result from dispersion of the dye due to diffusion, resulting in a estimated flowrate that exceeded the actual flowrate

A flow totalizer provided the volume of solution injected during the time period between injection rate measurements The number of days the system operated in this period was estimated by dividing the injected volume by the measured injection rate If

the result was greater than the number of days between two monitoring dates, the system was assumed to have operated continuously for the number of days between the two monitoring dates Time-weighted averages of injection rate, ($Q_{t,avg}$), at the wells during each period were determined as follows

$$Q_{t,avg} = ( \Sigma Q_i t_i )/( \Sigma t_i ) \quad (4\ 1)$$

where $t_i$ is the estimated period of operation at an injection rate $Q_i$

During Period I, the injection rate into SAD2 ranged from 2 5 to 5 8 L/min, with a time-weighted average of 1 65 L/min In contrast, the injection rate into SAD4 varied between 0 008 and 0 18 L/min, with a time-weighted average of 0 08 L/min During Period II, the injection rate into SAD2 ranged from 0 82 to 6 6 L/min, with a time-weighted average of 4 36 L/min, whereas the injection rate into SAD4 ranged from 0 005 to 0 09 L/min, with a time-weighted average of 0 02 L/min

During Period III, limited data were available from both wells as the system was mostly inoperational The arithmetic mean of injection rates was taken for this period The mean injection rate was 2 8 L/min at SAD2 and 0 02 L/min at SAD4, and the system was estimated to be in operation for 10 days Table 4 3 summarizes the average injection rates at the wells and the volumes injected The injection rates at SAD2 were more than two orders of magnitude greater than those at SAD4 (Figure 4 5)

Table 4 3 Flow rates and volume injected during the 3 periods of operation

| Period | Estimated days of operation | [a] Total system vol injected (L) | Injection rate SAD2 (L/min) | [b] Vol injected SAD2 (L) | Injection rate SAD4, (L/min) | [b] Vol injected SAD4 (L) |
|---|---|---|---|---|---|---|
| I | 39 0 | 122,300 | 1 65 | 92,600 | 0 08 | 440 |
| II | 75 3 | 496,900 | 4 36 | 472,300 | 0 02 | 1,640 |
| III | 10 0 | 42,200 | 2 71 | 39,000 | 0 02 | 310 |

[a] Based on flow totalizer readings

[b] Based on average injection rate to the well and estimated days of operation

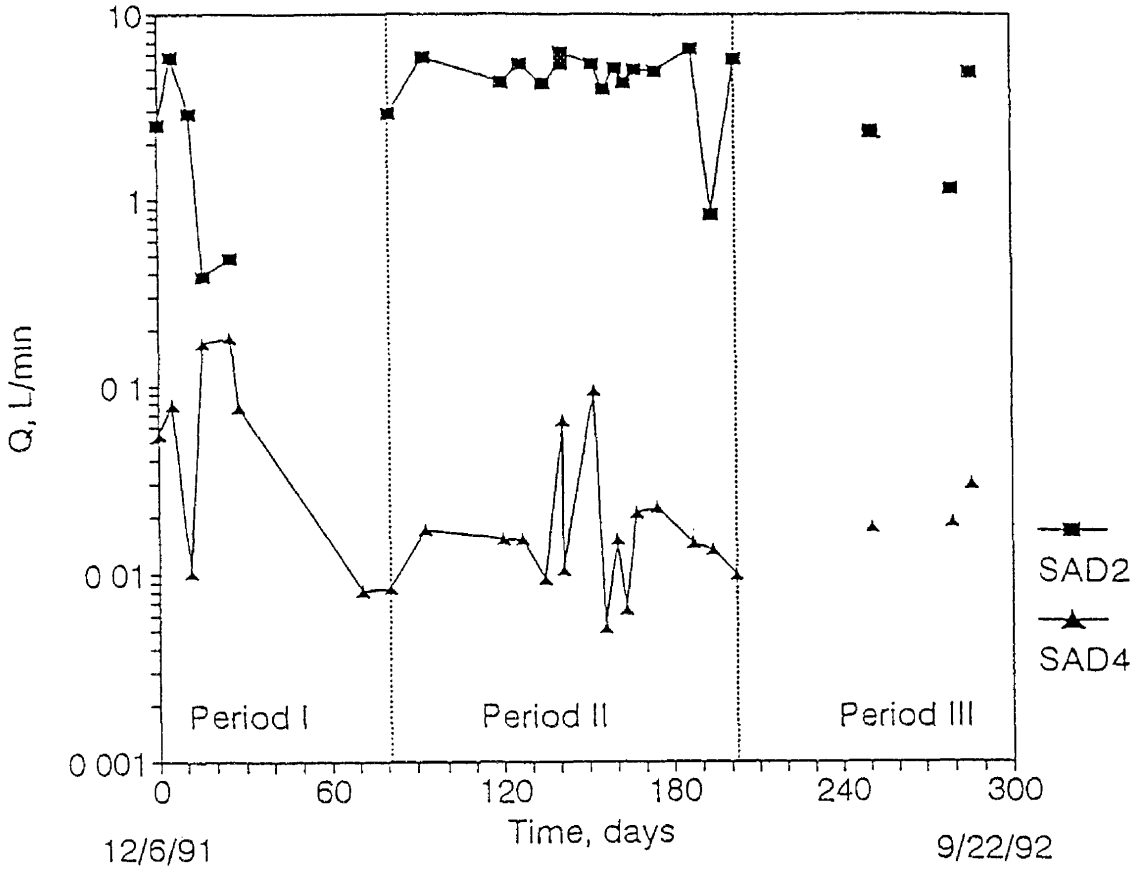


Figure 4 5 Injection rates for SAD2 and SAD4

### 4.8.4 Soil Moisture Contents

Moisture content data for the initial sampling episode were obtained by taking one 2 5-cm-long sample from each core for analysis Baseline moisture contents were fairly consistent at each sampling location and depth, ranging from 9 3 to 15%, with an average of 10 4% (std dev 1 26%)

During the second and third sampling episodes, the bottom 14 cm of the core was utilized for other analyses and the remainder of the core was divided into 2 5-cm-long sections for moisture content analysis, providing greater resolution of the moisture content with depth When sample recovery was 100%, the portion of the core available for moisture content was 46 cm, which provided eighteen 2 5-cm-long samples

When sample recovery was less than 100% (a common occurrence during split-spoon sampling), moisture contents for the missing section of the core were assigned the value of the section of recovered core in closest proximity to the missing section For example, if there was no recovery from a depth of 85 to 95 cm, the moisture content for the region from 85 to 90 cm was assigned the value obtained for a depth of 84 cm, and the region from 90 to 95 cm was assigned the value obtained for a depth of 96 cm These data were then plotted to provide profiles of moisture content with depth

**Vertical profile of soil moisture contents**

The moisture contents detected during the second and third sampling rounds were typically greater at regions close to fractures in the vicinity of SAD2 (Figures 4 6 and 4 7) During sampling in February, 1992, the moisture contents at SAD2-5 (located 1 5 meters from the well) were typically 10 to 25% with a peaks of 41% in the vicinity of a fracture at a depth of 1 4 m The moisture contents at SAD2-10 (located 3 meters from the well) and SAD2-15 (located 4 6 meters from the well) were typically 10 to 13% with a peak of 25% at depths of 1 4 to 1 6 m at SAD2-15 Moisture contents in the vicinity of SAD2 ranged from 10 to 25% during July, 1992

In contrast, moisture contents at SAD4-5 during sampling in February, 1992, were typically 8 to 14% with a maximum of 24% at a depth of 1 22 m The moisture contents at SAD4-10 and SAD4-15 were in the range of 8 to 13% Moisture contents in the vicinity of SAD4 were in the range of 9 to 12% during sampling in July, 1992 (Figure 4 7 and 4 8)

**Horizontal profile of soil moisture contents**

The moisture content data were used to obtain an integral mean value ($M_k$) for depth intervals of 1 2-1 8 m, 1 8-2 4 m, 2 4-3 0 m, and 3 0-3 7 m, as follows

$$M_k = \Sigma\, m_i * h_i / \Sigma\, h_i \quad (5\ 2) \qquad (4\ 2)$$

for $i$=1 24, $k$=1 2-1 8 m, 1 8-2 4 m, 2 4-3 0 m,

and 3 0-3 7 m where $h_i$ = 2 54 cm and $m_i$ = moisture content at $h_i$

The moisture content at SAD2-5 increased from 10% in September, 1991 to 25% in February, 1992 The sampling in July, 1992, indicated that moisture contents at SAD2-5 decreased to between 10 and 20% At SAD2-10 and SAD2-15, the moisture content showed negligible change in February, but had increased by July, 1992, indicating that the injected water affected moisture contents in those regions sometime between February and July, 1992

In contrast, only a slight change in moisture content was observed in the vicinity of SAD4 The moisture contents were in the range of 9 to 10% in the sampling of September, 1991, and increased to a range of 10 to 13% in the sampling of February, 1992, and were in the range of 9 to 12% in the sampling of July, 1992 Moisture content as a function of distance from the well is summarized in table 4 4

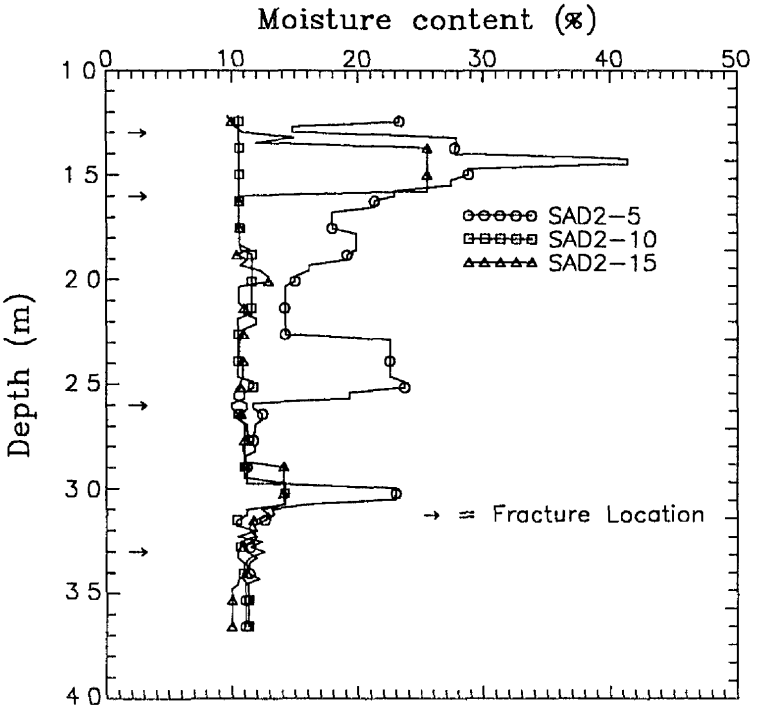


Figure 4 6 Vertical profile of moisture content in the vicinity of SAD2 (2/92)

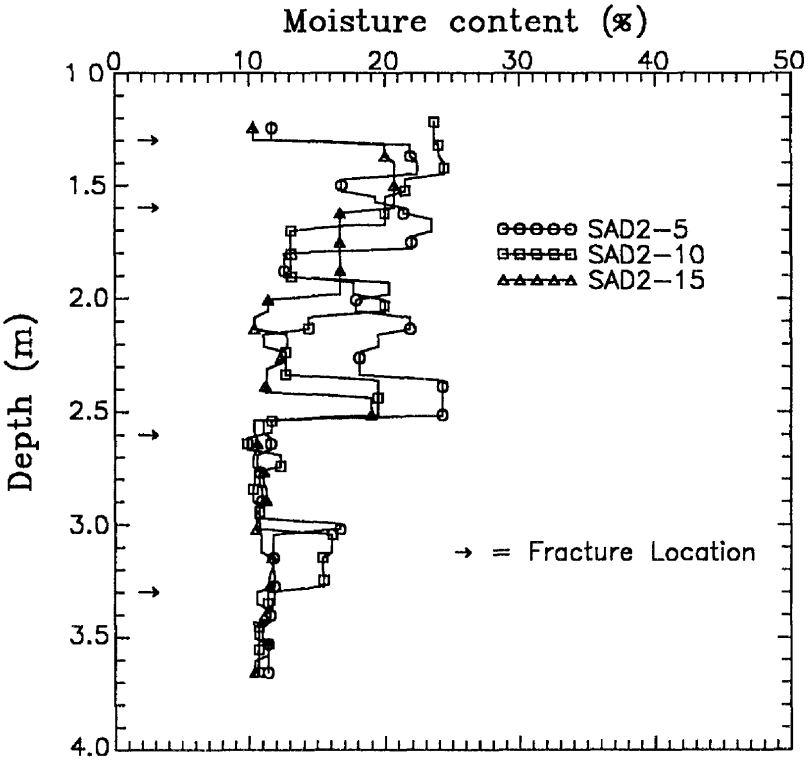


Figure 4 7 Vertical profile of moisture contents in the vicinity of SAD2 (7/92)

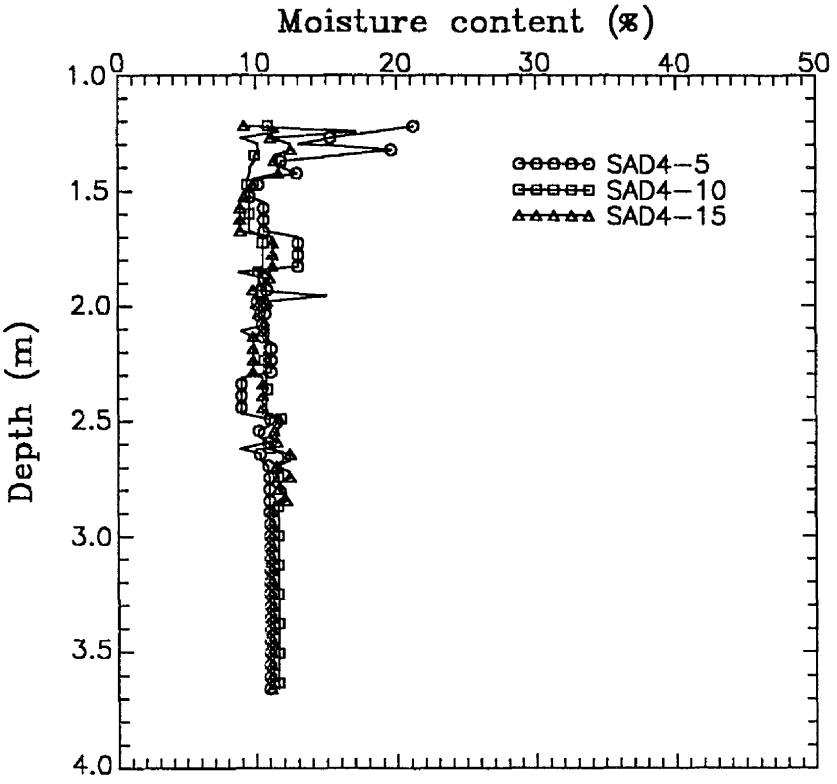


Figure 4 8 Vertical profiles of moisture contents in the vicinity of SAD4 (2/92)

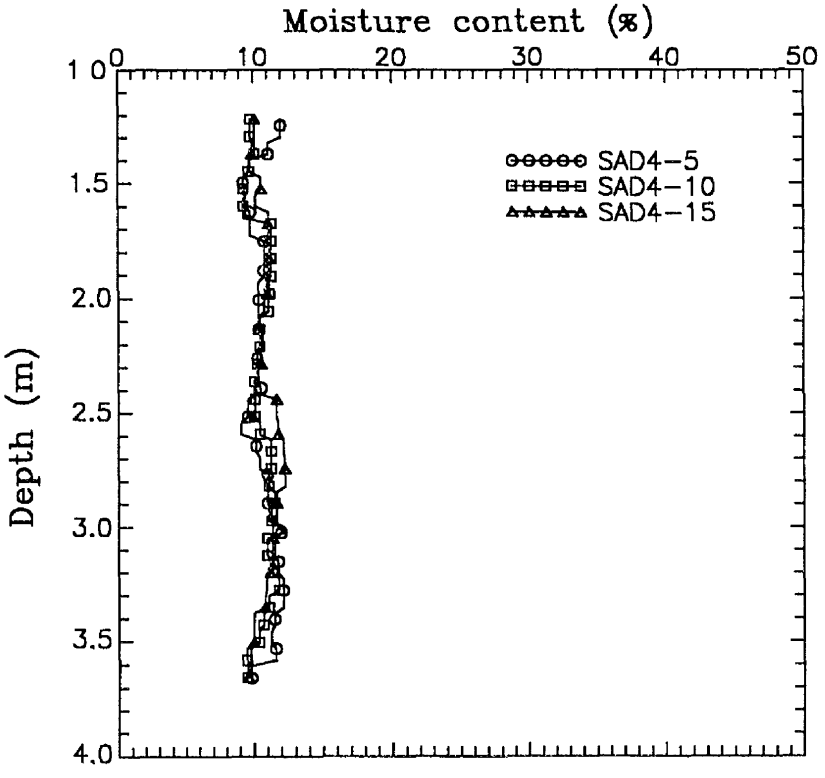


Figure 4 9 Vertical profiles of moisture contents in the vicinity of SAD4 (7/92)

Table 4 4 Horizontal profile of moisture contents in the vicinity of SAD2 and SAD4

| Sample location | Distance from well (meters) | Depth range (meters) | Moisture content % | | |
|---|---|---|---|---|---|
| | | | Sept | Feb | July |
| SAD2-5 | 1.52 | 1.2 to 1.8 | 11.3 | 24.2 | 19.6 |
| SAD2-5 | 1.52 | 1.8 to 2.4 | 10.8 | 17.4 | 18.1 |
| SAD2-5 | 1.52 | 2.4 to 3.0 | 9.9 | 15.0 | 13.6 |
| SAD2-5 | 1.52 | 3.0 to 3.7 | 9.9 | 12.3 | 11.5 |
| SAD4-5 | 1 52 | 1 2 to 1 8 | 9 6 | 12 9 | 10 2 |
| SAD4-5 | 1 52 | 1 8 to 2 4 | 10 5 | 10 4 | 10 5 |
| SAD4-5 | 1 52 | 2 4 to 3 0 | 10 5 | 10 6 | 10 5 |
| SAD4-5 | 1 52 | 3 0 to 3 7 | 10 5 | 11 0 | 11 5 |
| SAD2-10 | 3.05 | 1.2 to 1.8 | 10.6 | 10.6 | 21.9 |
| SAD2-10 | 3.05 | 1.8 to 2.4 | 11.0 | 11.1 | 14.3 |
| SAD2-10 | 3.05 | 2.4 to 3.0 | 11.8 | 11.4 | 12.3 |
| SAD2-10 | 3.05 | 3.0 to 3.7 | 11.8 | 11.3 | 13.0 |
| SAD4-10 | 3 05 | 1 2 to 1 8 | 9 3 | 10 0 | 9 5 |
| SAD4-10 | 3 05 | 1 8 to 2 4 | 9 3 | 10 5 | 10 7 |
| SAD4-10 | 3 05 | 2 4 to 3 0 | 9 3 | 11 5 | 11 1 |
| SAD4-10 | 3 05 | 3 0 to 3 7 | 9 3 | 11 6 | 10 7 |
| SAD2-15 | 4.57 | 1.2 to 1.8 | 15.0 | 16.4 | 18.9 |
| SAD2-15 | 4.57 | 1.8 to 2.4 | 9.4 | 11.1 | 13.1 |
| SAD2-15 | 4.57 | 2.4 to 3.0 | 9.4 | 11.7 | 12.1 |
| SAD2-15 | 4.57 | 3.0 to 3.7 | 9.4 | 11.3 | 11.2 |
| SAD4-15 | 4 57 | 1 2 to 1 8 | 10 1 | 107 | 10 5 |
| SAD4-15 | 4 57 | 1 8 to 2 4 | 10 1 | 10 5 | 10 7 |
| SAD4-15 | 4 57 | 2 4 to 3 0 | 10 1 | 11 5 | 11 9 |
| SAD4-15 | 4 57 | 3 0 to 3 7 | 10 1 | 11 1 | 10 5 |

### 4.8.5 Bioactivity

Soil samples from the vicinity of the two wells were analyzed for FDA activity and microbial counts The following sections and Figures 4 9 through 4 12 describe the results of the three sampling episodes

**FDA Activity**

There was more microbial metabolic activity (FDA activity) in the soil around the hydraulically fractured well compared to that around the conventional well The microbial metabolism increased much more in the vicinity of the fractures than between fractures, and more than in the vicinity of the unfractured well

The greatest FDA activity was observed near the fractures at SAD2-5 The level of FDA activity declined at some locations, particularly in lower fractures, between the second and third sampling dates In contrast, the FDA activity at SAD4-5 was low and remained low during the treatment

Greater FDA activity was observed to depths of 2 1 m at SAD2-10 compared to those at greater depths This is the general area of greatest contamination and therefore the area where one would expect greatest microbial activity Insignificant changes in FDA activity were observed between the second and third sampling dates in the lower zone This may be due to the low level of contamination At SAD2-10S, the FDA activity was high initially, appeared to decline, and returned to initial levels by the time of the third sampling (Figure 4 12) At SAD4-10, the FDA activity was low and decreased in the third sampling No sampling was conducted 3 0 m south of SAD4 because of the original placement of the wells

At SAD2-15, the FDA activity increased in areas around most fractures by the time of the second sampling but declined by the third sampling At SAD4-15, there was no significant change in the FDA activity

**Microbial Counts**

The number of hydrocarbon degraders was perhaps the most variable of the factors considered in this study The soil profile indicated that a 10 to 100 fold variability through the soil column was common In most cases, there was a 10 to 100 fold increase in hydrocarbon degrader numbers in the soil in the vicinity of the fractures In general, the increases in hydrocarbon degraders correlated with increased metabolic activity As with the FDA activity, a decline in microbial numbers between the second and third samplings was observed for most areas in the study However, the overall decrease in those parameters was less for the hydraulically fractured well than for the conventional well

The number of hydrocarbon degraders at SAD2-5 increased by two orders of magnitude in most areas in the immediate vicinity of the fractures by the second sampling episode An increase of one order of magnitude was measured between the fractures However, the number of hydrocarbon degraders decreased by one to two orders of magnitude by the third sampling The number of hydrocarbon degraders at SAD4-5 showed insignificant change by the time of the second sampling and decreased during the third sampling

The population of hydrocarbon degraders at SAD2-10 was small except for occasional peaks adjacent to the fractures At SAD2-10S, the number of hydrocarbon degraders was low initially, increased approximately 10 to 100 times, then decreased or stayed the same by the third sampling At SAD4-10, the number of hydrocarbon degraders was similar to that at SAD2-10, and declined in the third sampling No sampling was conducted 3 0 m south of SAD4 because of the original placement of the wells

At SAD2-15, the number of hydrocarbon degraders increased around most fractures by the time of the second sampling but decreased during the third sampling At SAD4-15, the number of hydrocarbon degraders was low initially, increased by the second sampling, then declined greatly (10 to 100 fold) by the third sampling

### 4.8.6 Analytical Results

A summary of the chemical analyses of samples is given in Tables 5 4 and 5 5 Initial sampling indicated that most of the contamination was in the area covered by the fractured well at depths of 1 2 to 3 0 m

The contaminant distribution at this site is heterogeneous (Table 5 4) For example, ethylbenzene concentrations varied in the range of 15 to 26 ppm in the vicinity of SAD2 during the first sampling The number of samples required to obtain a true representation of the contaminant distribution would result in the destruction of the site by the sampling process itself The sampling procedure only gives us a picture of the soil column at various locations based on a series of point observations Thus, the chemical analyses only provide indicators of the performance of bioremediation

The percent reduction in the concentration of the contaminants were obtained from the initial and subsequent sampling analyses In many instances, the percent reduction in contaminant concentrations by the time of the third sampling was less than that during the second sampling, a trend that is similar to those of metabolic activity and microbial numbers We expected the contaminant concentrations to decrease or at least stay the same between the second and third sampling dates In some cases, however, the contaminant concentration in the third sampling was greater than that during the first sampling For example, at SAD2-10, there was a 72% decrease in BTE between the first and second sampling, and a 6% increase between the first and third sampling Increases in concentration between the first and subsequent sampling are reported as a 0% decrease in Table 4 5 There are a number of cases where the limited sampling has resulted in unexpected results

Comparison of samples at 1 5 m distance from the two wells yields the most meaningful information on the performance of the wells Samples at SAD2-5 showed an 80% decrease in benzene concentration, 60% reduction in ethyl benzene concentration, a 59 to 75% reduction in BTE concentration, and 71 to 77% reduction in TPH concentration (Table 4 5) In contrast, samples at SAD4-5 showed no change in benzene concentration, 26% reduction in ethyl benzene concentration, a 0 to 10% change in BTE concentration, and 0 to 55% reduction in TPH concentration Initial sampling indicated a high BTE concentration in the area 4 6 meters north of the fractured well There, the

BTE concentration in the samples showed a reduction of 45 to 69% and the TPH levels were reduced by 51 to 68% in subsequent samples

Table 4 5 Chemical analysis of split spoon samples from the Dayton site

| ID | Location | Sampling Episode | Avg Concentration (ppm) | | | |
|---|---|---|---|---|---|---|
| | | | Benzene | E Ben | Toluene | TPH |
| SAD2 | 1.5 m | 1st | 4.0 | 15.0 | 0.2 | 490 |
| | | 2nd | 4.4 | 0.4 | ND | 112 |
| | | 3rd | 0.8 | 6.0 | 1.0 | 143 |
| SAD4 | 1 5 m | 1st | 3 7 | 8 9 | 0 8 | 230 |
| | | 2nd | 4 9 | 8 1 | 1 6 | 235 |
| | | 3rd | 5 0 | 6 6 | 0 5 | 104 |
| SAD2 | 3.0 m | 1st | 6.0 | 20.0 | 0.5 | 235 |
| | | 2nd | 3.2 | 4.3 | ND | 98 |
| | | 3rd | 5.3 | 20.0 | 2.8 | 108 |
| SAD4 | 3 0 m | 1st | 0 8 | 2 1 | 0 1 | 75 |
| | | 2nd | 0 7 | 0 6 | ND | 55 |
| | | 3rd | 0 6 | 0 2 | 0 2 | 25 |
| SAD2 | 4.6 m | 1st | 9.8 | 26 | 1.2 | 385 |
| | | 2nd | 3.5 | 7.1 | 0.7 | 188 |
| | | 3rd | 6.1 | 11.4 | 2.7 | 123 |
| SAD4 | 4 6 m | 1st | 0 3 | 0 2 | ND | 8 |
| | | 2nd | 0 3 | ND | ND | 11 |
| | | 3rd | 0 7 | 0 7 | ND | 6 |
| SAD2 | 3.0 m S | 1st | 1.0 | 0.9 | ND | 290 |
| | | 2nd | 1.3 | ND | ND | 131 |
| | | 3rd | 0.9 | 2.3 | 1.1 | 57 |

*ND = not detected

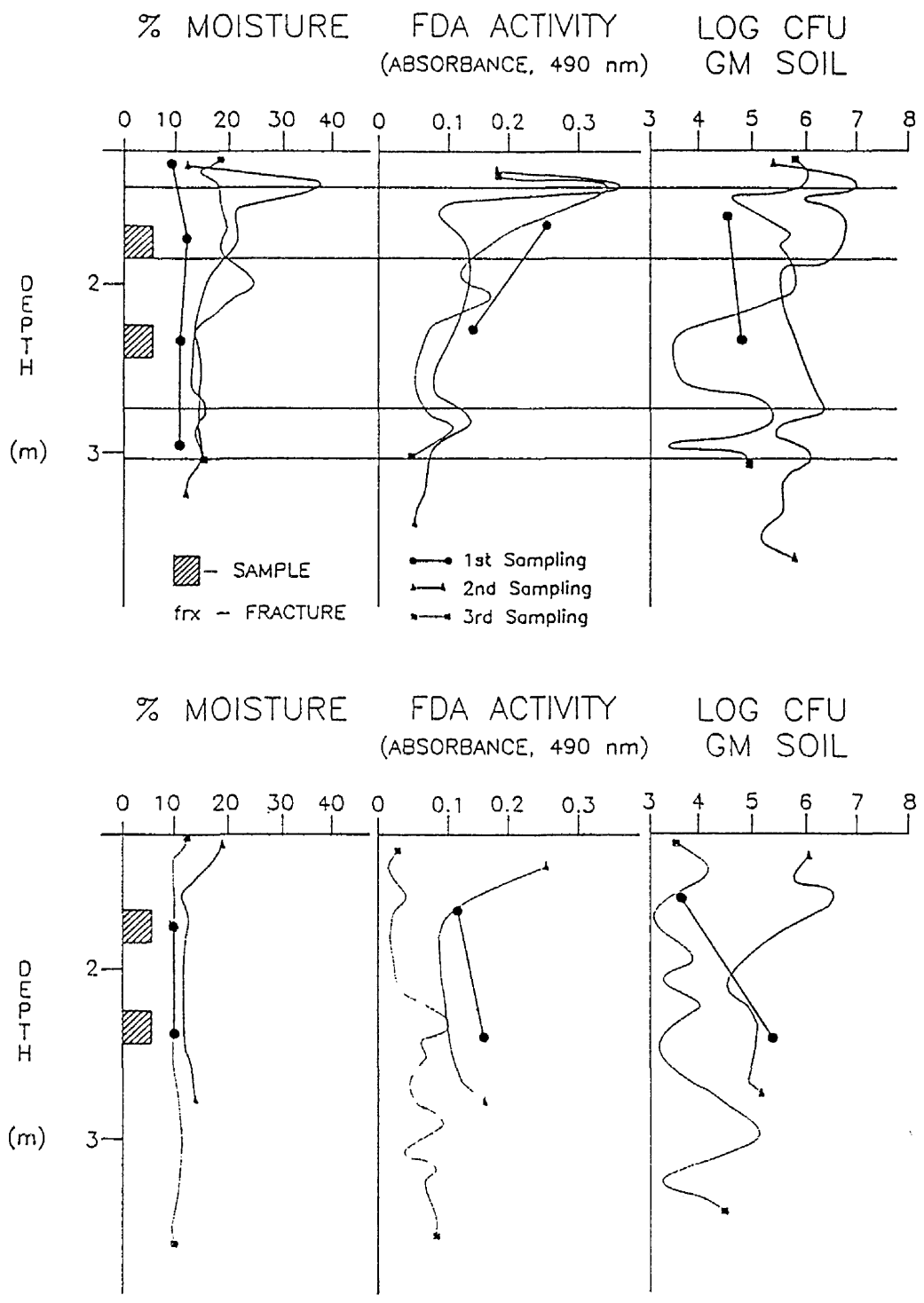


Figure 4 10 Moisture content, FDA activity, and microbial counts at SAD2-5 (top) and SAD4-5 (bottom)

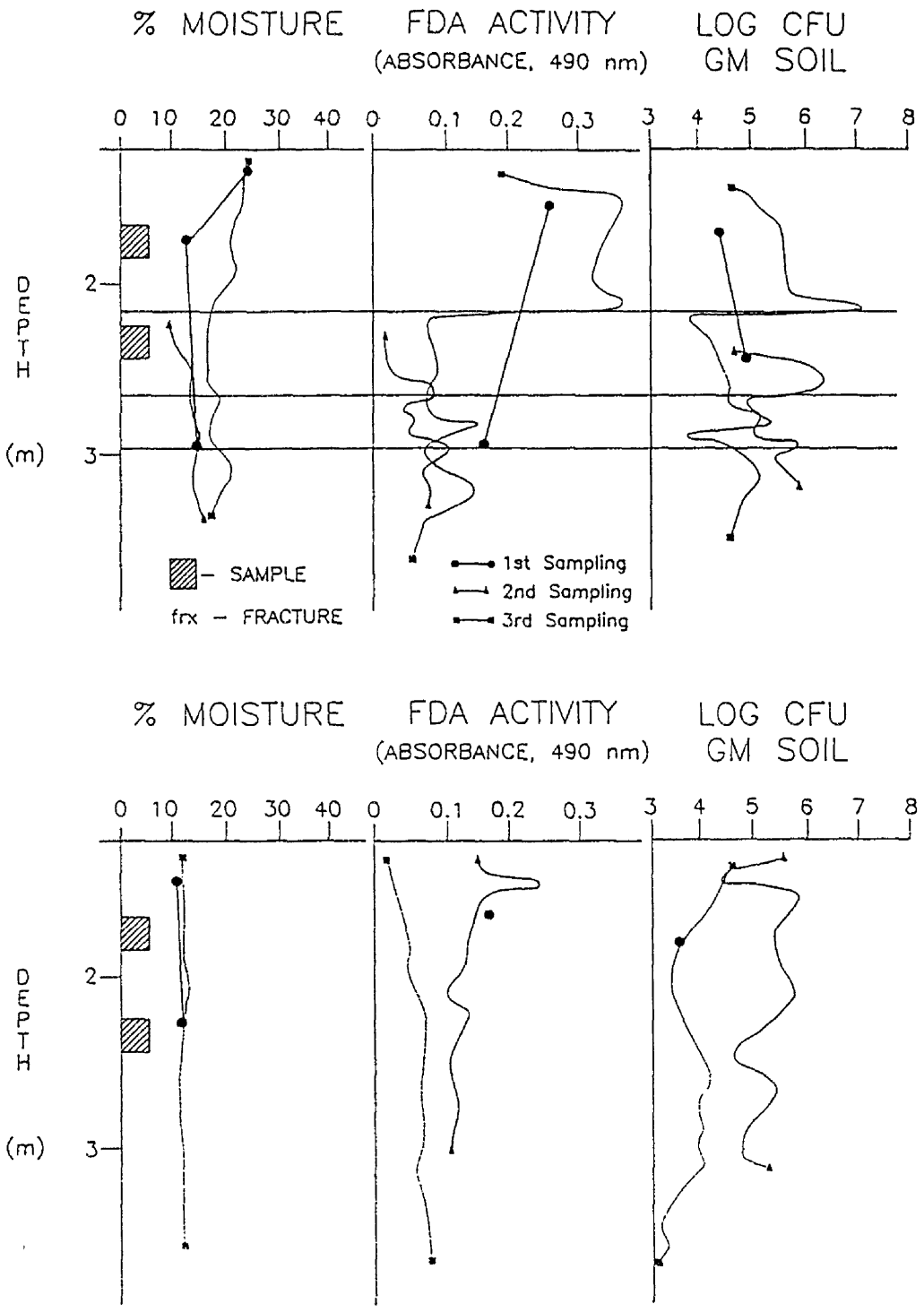


Figure 4 11 Moisture content, FDA activity, and microbial counts at SAD2-10 (top) and SAD4-10 (bottom)

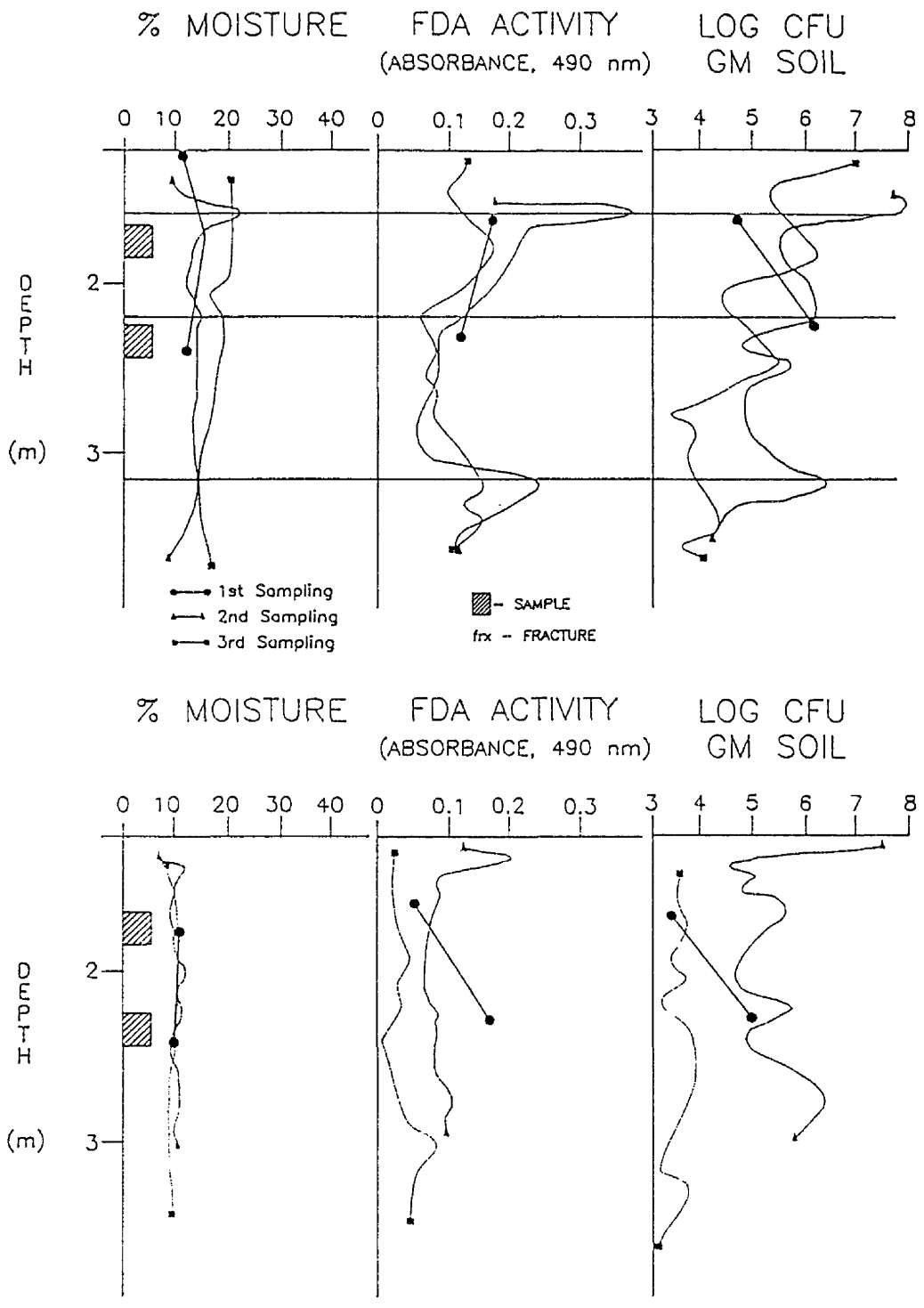


Figure 4 12 Moisture content, FDA activity, and microbial counts at SAD2-15 (top) and SAD4-15 (bottom)

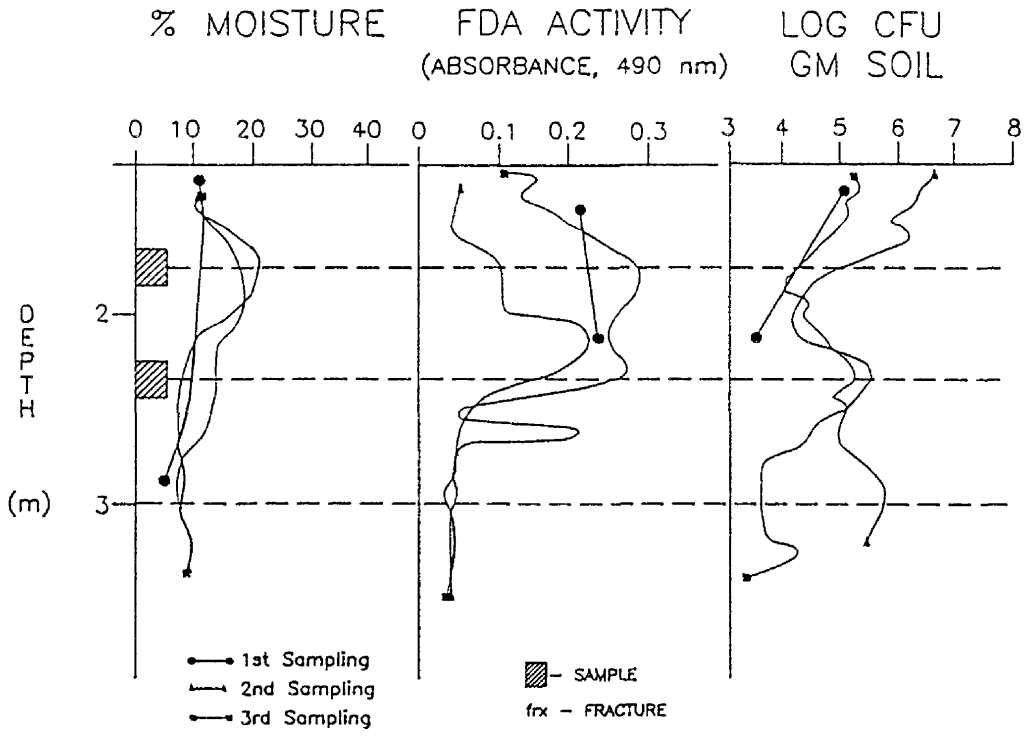


Figure 4 13 Moisture content, FDA activity, and microbial counts at SAD2-10S

Table 4 6 Total hydrocarbon removed based on concentration change between sampling events

| ID | Location | Sampling episode | BTE removed (mg/Kg) or % total | TPH removed (mg/Kg) or % total |
|---|---|---|---|---|
| SAD2 | 1.5 m | 2nd | 14.4 or 75% | 378 or 77% |
| | | 3rd | 11.4 or 59% | 347 or 71% |
| SAD4 | 1 5 m | 2nd | 0 or 0% | 0 or 0% |
| | | 3rd | 1 3 or 10% | 126 or 55% |
| SAD2 | 3.0 m | 2nd | 19 or 72% | 137 or 58% |
| | | 3rd | 0 or 0% | 127 or 54% |
| SAD4 | 3 0 m | 2nd | 1 7 or 57% | 20 or 27% |
| | | 3rd | 2 or 67% | 50 or 67% |
| SAD2 | 4.6 m | 2nd | 25.7 or 69% | 197 or 51% |
| | | 3rd | 16.8 or 45% | 262 or 68% |
| SAD4 | 4 6 m | 2nd | 0 2 or 40% | 0 or 0% |
| | | 3rd | 0 or 0% | 2 or 25% |
| SAD2 | 3.0 m S | 2nd | 0.6 or 60% | 159 or 55% |
| | | 3rd | 0 or 0% | 233 or 80% |

## 4.9 Summary

The significant results of this study are

1) The injection rate at the fractured well SAD2 was more than two orders of magnitude greater than the conventional well SAD4

2) Subsurface pressure head was higher in the vicinity of SAD2, particularly along the fractures, than in the vicinity of SAD4

3) The moisture contents increased in the vicinity of fractures Sampling in February showed a significant increase in moisture content occurred beyond 1 5 m from SAD2 Moisture contents increased significantly at a distance 4 6 m from the SAD2 during sampling in July In contrast, only a slight change in moisture content was observed at the control well during sampling in February and July

4) Microbial population and metabolic activity increased between the first and second sampling with a corresponding decrease in contaminant concentrations However, microbial population and activity decreased between the second and third sampling, and in

some samples, those parameters were less in the third sampling than in the first sampling The decrease in microbial population and activity between the second and third samplings can be attributed to several factors related to operation of the injection system and unrelated to the performance of hydraulic fractures

5) There was more metabolic activity (FDA activity) in the soil in the vicinity of the hydraulically fractured well compared to the conventional well

6) There was a 10 to 100 fold increase in hydrocarbon degraders in the vicinity of the fractures In general, the increases in hydrocarbon degraders correlated with increased metabolic activity

# 5.0 Summary

The study described here focused on identifying and quantifying the effects of hydraulic fracturing during SVE and in situ bioremediation Results indicate that under the modest suctions (127 cm $H_2O$) used during the Center Hill study, the average discharge was 130 L/min at the fractured wells whereas the average discharge was 13 L/min at the conventional wells Similar results occured using higher suction head (690 cm $H_2O$) at the Xerox site, where the average discharge was 522 L/min from the fractured wells (when suction was not applied to the vented fracture at RW4) whereas it was 31 L/min from the conventional well

Water was recovered more rapidly during SVE from fractured wells than from control wells Fractured wells at both the Center Hill site and the Xerox site consistently produced water after precipitation events, whereas the conventional wells rarely produced water Moisture in soil pores limits the flow of air through soil, so removal of water from soil pore space is imperative when performing SVE

In addition to increasing the well discharge, hydraulic fractures also increased the area influenced by a well A suction head of 2 5 cm $H_20$ suction was consistently measured at distances greater than 4 5 meters, and in many cases at distances as great as 7 5 meters, from the fractured wells In contrast, suction head in the vicinity of the conventional wells was rarely detectable more than 1 meter from the well

At the Xerox site, the greater well discharges associated with the fractured wells were accompanied by greater mass recovery rates The contaminant mass recovery rate for the fractured wells ranged from 7 to 14 times greater than from the conventional well

At the Dayton bioremediation site, the infiltration rate of nutrients and oxygen at the fractured well was two orders of magnitude greater than the conventional well Increases in subsurface pressure head and moisture content in the vicinity of the fractured well was accompanied by an increase in bioactivity and reductions in contaminant concentration Effects were particularly evident in the immediate vicinity of the fractures, presumably the areas between the fractures would have received the same benefits had the system run more consistently/for a longer duration

This study demonstrated that sand-filled hydraulic fractures increase subsurface flow and the areas affected by wells by an order of magnitude or more It presents preliminary data that indicate increases in flow are accompanied by an increase in remediation rate The increase in the area affected reduces the number of wells required, thereby reducing drilling, well completion, and cuttings disposal cost In addition, increasing the rate of remediation reduces monitoring and utility cost

# 6.0 References


Dames and Moore, 1990 *Initial Reevaluation of the Extent of Vertical Contamination at the Oakbrook Xerox Corporation, Oakbrook, Illinois*, Draft report

Golder Associates, 1986, *Contaminant Hydrogeologic Investigation at the Xerox PR&S Facility, Oakbrook, Illinois,* Volume I August, 1986, Draft report

Leahy, J H and R R Colewell 1990 *Microbial Review.* 54 305-325

Murdoch, L, G Losonsky, P Cluxton, B Patterson, I Klich, B Brasswell (1991a), *The Feasibility of Hydraulic Fracturing of Soil to Improve Remedial Actions: Final Report.* USEPA 600/2-91-012 NTIS report PB91-181818 298

Murdoch, L , W Slack, M Kemper, P Cluxton, D Kreuzmann, (1991b), *Hydraulic Fracturing to Facilitate Remediation . Phase I, Interim Report* Center for GeoEnvironmental Science and Technology, University of Cincinnati, Cincinnati, Ohio

Murdoch, L , M Kemper, A Wolf (1992) *Hydraulic Fracturing to Improve Delivery and Recovery* Proceedings of the 1992 USEPA/A&WMA International Symposium, In Situ Treatment of Contaminated Soil and Water

Ryan, J R , R C Loehr, and E Rucker 1991 "Bioremediation of Oganic Contaminated Soils", *Journal of Hazardous Materials* 28 159-169

Schnurer, J and T Rosswall 1985 *Applied Environmental Microbiology* 43 1256-1261

USEPA, 1983 *Methods for Chemical Analysis of Water and Wastes* USEPA EPA-600/4-79-020 Environmental Monitoring Systems Laboratory, Washington, D C

USEPA, 1990 *Test Methods for Evaluating Solid Wastes, Physical/Chemical Methods. SW-846* Office of Solid Waste and Emergency Response, 3rd Ed , Washington, D C

Vesper, S J , L C Murdoch, S Hayes, and W J Davis-Hoover 1993 "Solid Oxygen Source for Bioremediation in Subsurface Soils" *Journal of Hazardous Materials* Accepted